

Lawrence Berkeley National Laboratory

LBL Publications

Title

Light-driven anaerobic microbial oxidation of manganese

Permalink

<https://escholarship.org/uc/item/7684d26c>

Journal

Nature, 576(7786)

ISSN

0028-0836

Authors

Daye, Mirna

Klepac-Ceraj, Vanja

Pajusalu, Mihkel

et al.

Publication Date

2019-12-12

DOI

10.1038/s41586-019-1804-0

Peer reviewed

1 **Light-Driven Anaerobic Microbial Oxidation of Manganese**

2 Mirna Daye¹, Vanja Klepac-Ceraj², Mihkel Pajusalu¹, Sophie Rowland², Anna Farrell-Sherman²,
3 Nicolas Beukes³, Nobumichi Tamura⁴, Gregory Fournier¹, Tanja Bosak¹

4 **Affiliations:**

5 ¹Department of Earth, Atmospheric, and Planetary Sciences, Massachusetts Institute of
6 Technology, Cambridge, Massachusetts 02139.

7 ²Department of Biological Sciences, Wellesley College, 106 Central St, Wellesley,
8 Massachusetts 02481.

9 ³DST-NRF CIMERA, Geology Department, University of Johannesburg, Auckland Park, 2006,
10 South Africa.

11 ⁴Advanced Light Source, Lawrence Berkeley National Laboratory, Berkeley, California 94720,
12
13

14 **Oxygenic photosynthesis supplies organic carbon to the modern biosphere, but it is**
15 **uncertain when this metabolism originated. Based on the inferred presence of manganese**
16 **oxides in the sediments as old as 3 billion years, it has been proposed that photosynthetic**
17 **reaction centers capable of splitting water arose by that time. However, this assumes that**
18 **manganese oxides can only be produced in the presence of molecular oxygen¹, reactive**
19 **oxygen species^{2,3} or by high-potential photosynthetic reaction centers^{4,5}. Here we show that**
20 **anoxygenic photosynthetic microbial communities biomineralize manganese oxides under**
21 **strictly anaerobic conditions and in the absence of high-potential photosynthetic reaction**
22 **centers. Microbial oxidation of Mn(II) in the absence of molecular oxygen during the**
23 **Archean Eon would have produced geochemical signals identical to those used to date the**
24 **evolution of oxygenic photosynthesis before the Great Oxidation Event (GOE)^{6,7}. This light-**
25 **dependent process may also produce manganese oxides in the photic zones of modern**
26 **anoxic water bodies and sediments.**

27 Manganese (Mn) and more than 30 of its described oxides and hydroxides mediate the cycling of
28 various trace metals and nutrients in the environment. The ability of microbes to oxidize Mn(II)
29 anaerobically is also hypothesized to have been a critical step in the evolution of oxygenic
30 photosynthesis on the early Earth⁴. However, modern microbes are not known to anaerobically
31 oxidize manganese. Here, we demonstrate this activity in active microbial cultures that grow in
32 the presence of nanomolar oxygen concentrations relevant for the Archean Earth.

33 Inoculum for the enrichment cultures of strictly anaerobic, photosynthetic biofilms came
34 from the meromictic Fayetteville Green Lake (FGL), NY. The anaerobic photic zone of the lake
35 contains 20 nM to 61 μ M Mn(II) and 0-0.04 mM of H₂S [8], and the most abundant phototroph
36 there is the green sulfur bacterium *Chlorobium* sp.⁹. This microbe uses sulfide, hypothesized to
37 be the oldest electron donor for photosynthesis¹⁰, as an electron donor. Photosynthetic biofilms of
38 this organism and other strict anaerobes (Fig. 1a) were enriched in a minimal medium amended
39 with 20-50 μ M Na₂S and 1 mM MnCl₂ and equilibrated with an anaerobic atmosphere of 80% N₂
40 and 20% CO₂ at pH 7. The concentration of O₂ in the medium was lower than 2 nM during the
41 entire experiment, both in the presence and the absence of cells (see Methods and Extended Data
42 Fig. 1). These experimental concentrations match the upper estimates for the Archean Earth¹¹.
43 The anaerobic medium also lacked other potential oxidants for Mn(II) such as nitrite, nitrate and
44 H₂O₂ and these species were not produced in sterile controls (Extended Data Section 5).

45 Four times more biomass grew in photosynthesizing cultures relative to the cultures
46 incubated in the dark (p -value $\ll 0.001$; Fig. 1b). The enrichment protocol removed all typical
47 biological sources of oxygen such as cyanobacteria and photosynthetic eukaryotes from the
48 original inoculum and all of the subsequent transfers (Fig. 1c). The resulting community was
49 stable and contained *Chlorobium*, *Paludibacter*, *Acholeplasma*, *Geobacter*, *Desulfomicrobium*,
50 *Clostridium*, *Acetobacterium*, and several other bacteria. The *Chlorobium* sp. was the most
51 abundant taxon across all conditions, as well as the only identifiable phototroph (Fig. 1c). Its
52 genome was 98.4% similar to *Chlorobium limicola* Frassasi.

53 These microbial communities were essential to the precipitation of minerals and
54 oxidation of manganese. Mn-rich dolomite was the most abundant precipitate in photosynthetic
55 cultures amended with 0.1-1 mM Mn(II) and 20-250 μ M sulfide (Fig. 2, Extended Data Fig. 5a,
56 b, d)¹⁴, which is in the 0.1 mM range of dissolved Mn(II) concentrations thought to have been
57 maintained by precipitation of Mn-containing carbonate minerals on the Archean carbonate
58 platforms^{12,13}. Cultures incubated in this range of chemical conditions also contained manganese
59 oxide minerals (Figs. 1d, 2), but those incubated with ~ 1 μ M Mn(II) or 1 mM sulfide did not
60 (Extended Data Fig. 5c). Precipitates were entirely absent from sterile controls incubated in the
61 light, whereas minor calcite, less dolomite and no manganese oxides were detected in cultures
62 shielded from the light (Fig. 2). Elemental S⁰ accumulated in cultures that did not contain
63 oxidized manganese minerals (Extended Data Figs. 5c and 6), as expected when *Chlorobium* sp.
64 grows on sulfide as the main photosynthetic electron donor (Extended Data Fig. 7). The lack of
65 oxidized manganese in sterile controls showed that abiotic oxidation reactions did not contribute
66 detectable amounts of manganese oxides under our experimental conditions. Thus, the microbial
67 presence and photosynthetic activity strongly controlled the nucleation and precipitation of
68 minerals, including manganese oxides, under our experimental conditions.

69 To characterize the redox cycling of manganese, we examined its oxidation state by
70 surface-sensitive methods (Extended Data Figs. 2, 3). After two weeks, sterile controls and
71 cultures that were incubated in the dark contained only Mn(II) (Extended Data Figs. 2 and 3a).
72 Dolomite that formed in photosynthetic cultures contained Mn(II)¹⁴, but Mn(II), Mn(III) and
73 Mn(IV) in calcium manganese oxides, Mn₃O₄ and other minerals were also detected (Figs. 1d, 2;
74 Fig. 3, Extended Data Figs. 3, 4). The presence of manganese oxides in sulfidic photosynthetic
75 cultures was surprising (Fig. 2), but we detected them repeatedly in biofilms that were two weeks
76 to two months old (Fig. 2). A colorimetric assay quantified 5.1 ± 0.8 μ M of oxidized manganese
77 in one-week-old biofilms, 7.2 ± 0.8 μ M oxidizing equivalents in two-week-old biofilms to > 10
78 μ M in three-week old biofilms (Methods 6). All oxidized manganese was determined as KMnO₄
79 equivalents and none was detected in dark controls.

80 Oxidized manganese was present in minerals that formed directly at the surfaces of cells
81 (Fig. 3a). These cells could be identified as *Chlorobium* sp. based on the presence of large
82 intracellular complexes of photosynthetic antennae called chlorosomes (Fig. 3b) and surface
83 protrusions called spinae¹⁵. Notably, minerals were only found on cell surfaces and never around
84 chlorosomes, pointing to the involvement of cell surfaces and periplasmic processes in
85 manganese oxidation. High-resolution transmission electron micrograph of fresh cell suspensions
86 showed Mn-Ca minerals with a uniform lattice fringe that corresponded to (121) plane with
87 interplanar spacing of 2.64 Å of calcium manganese oxide (Fig. 3d), Mn₃O₄ (Fig. 3f) and other
88 manganese minerals (Extended Data Fig. 3, 4). Extracellular vesicles, spinae and manganese

89 oxide minerals were absent from *Chlorobium* sp. when the cultures were incubated with Mn(II)
90 in the dark or photosynthetically with 1 mM sulfide.

91 Light-driven manganese oxidation occurred only when *Chlorobium* sp. and other
92 microbes, including *Geobacter* sp., were growing together. Oxidized manganese was present in
93 enrichment cultures of microbes from FGL that contained *Chlorobium* sp, *Geobacter* sp.,
94 *Acholeplasma equifetale*, *Alistipes* sp. HGB5, and *Caldicoprobacter oshimai*, but absent from
95 co-cultures of *Chlorobium* sp. and *Desulfomicrobium* sp. (Extended Data Fig. 8) and pure
96 cultures of *Chlorobium limicola*. To identify the simplest co-cultures that could oxidize
97 manganese, we tested for the presence of manganese oxidizing activity in co-cultures of isolated
98 strains of *C. limicola*, *Chlorobaculum tepidum* and *Geobacter lovleyi* (DSM 245, DSM 12025
99 and DSM 17278, DSMZ GmbH Germany) (Extended Data 2.3.1). Manganese oxidizing activity
100 was detected only in the co-cultures containing all three organisms and the co-cultures of *C.*
101 *limicola* and *G. lovleyi* (Extended Data Fig. 9), suggesting that the activity may depend on
102 extracellular electron transfer between the latter two organisms¹⁶ by a currently unknown
103 mechanism. The genome of *Chlorobium* sp. encodes only a well-studied photosynthetic reaction
104 center with the midpoint potential around +250 mV¹⁷ that cannot directly oxidize Mn(II)-
105 bicarbonate (Eh = 520-670 mV)^{4,18}. *Chlorobium* sp. also lacks clear homologs of proteins known
106 to oxidize manganese under aerobic conditions¹⁹⁻²¹. Manganese oxidation in *C. limicola* may
107 occur by an endergonic mechanism analogous to that proposed for the oxidation of nitrite by
108 *Thiocapsa* sp. strain KS1²², but Mn(II) oxidation process and potential oxidants in the co-cultures
109 of *C. limicola* and *G. lovleyi* remain to be characterized. The electron transfer between *C.*
110 *limicola* and *G. lovleyi* may involve high potential cytochrome c in *Chlorobium* sp. and OmpB
111 operating in reverse in *Geobacter* sp.

112 The abundance of oxidized manganese in microbial biofilms and its absence from the
113 sterile controls shows that microbial consortia can mediate the precipitation of manganese oxide
114 minerals under Archean-like conditions. These findings expand the diversity of minerals and
115 redox processes beyond what was thought possible in strictly anaerobic environments or in the
116 presence of high-potential photosynthetic reaction centers. Microbial interactions that mediate
117 the light-dependent redox cycling of manganese and couple it to other elemental cycles remain to
118 be identified, but can be expected in modern environments where light, sulfide and dissolved
119 Mn(II) coexist, but sulfide concentrations do not exceed ~ 0.2 mM (Extended Data Table 1).
120 Light dependent microbial production of manganese oxides is likely to stimulate the redox cycles
121 of carbon, sulfur, nitrogen and iron and increase the diversity of anaerobic redox transformations,
122 including nitrification-denitrification²³, with implications for the interpretation of isotopic and
123 chemical signatures of these processes in modern anaerobic settings.

124 The biological production of manganese oxides under Archean-like chemical conditions
125 has additional major implications for determining the timing of the origin of oxygenic
126 photosynthesis, which is currently debated⁵⁻⁷. The evolution of oxygenic photosynthesis⁶ and the
127 presence of locally oxic areas in the pre-GOE, Archean marine systems²⁴ are inferred from
128 geochemical signals. However, interpretations of these signals assume the former presence of
129 manganese oxides^{6,7,25,26}. For example, manganese carbonate deposits with the negative $\delta^{13}\text{C}$
130 values reported in the Neoproterozoic Sandur Schist belt in India²⁷ or Mesoproterozoic Witwatersrand-
131 Mozaan strata in South Africa^{24,25} are thought to have been produced by the microbial reduction
132 of Mn(III) and Mn(IV)-oxide minerals. In turn, these oxides are attributed to the aerobic

133 oxidation of Mn(II) in the presence of oxygen. Molecular clock models are used to
134 independently time the evolution of the crown group cyanobacteria, with estimates that range
135 from before 3 billion years ago (Ga) to after the GOE, depending on sequence datasets, prior
136 assumptions and specific model calibrations²⁸. These models support the radiation of anoxygenic
137 green sulfur bacteria (GSB) such as *Chlorobium* and green non-sulfur bacteria (GSN) after the
138 GOE²⁸, but also show that stem GSB diverged as early as 2.9 Ga. Given that the last common
139 ancestor of modern GSB was photosynthetic, model estimates are consistent with anoxygenic
140 photosynthesis within stem GSB long before the GOE (also see Extended data Fig.
141 11). Therefore, given that anaerobic manganese oxidation requires anoxygenic photosynthetic
142 activity in the presence of sulfide, this process could be as old as anoxygenic phototrophic
143 ancestors of any extant groups of phototrophs, such as GSB, Cyanobacteria, or even an extinct
144 lineage of anoxygenic phototrophs. Because any of these scenarios can predate the GOE, the
145 relative contributions of anaerobic and oxygen-dependent Mn(II) oxidation to the redox texture
146 of sedimentary rocks much before the GOE²⁹ are an open question and the loss of mass-
147 independent sulfur isotope signals at GOE³⁰ remains the firmest evidence for biological
148 production of oxygen.

149

150 **References**

- 151 1 Tebo, B. M. *et al.* Biogenic manganese oxides: properties and mechanisms of formation.
152 *Annu. Rev. Earth Planet. Sci.* **32**, 287-328 (2004).
- 153 2 Oze, C., Sleep, N. H., Coleman, R. G. & Fendorf, S. Anoxic oxidation of chromium.
154 *Geology* **44**, 543-546 (2016).
- 155 3 Liang, M.-C., Hartman, H., Kopp, R. E., Kirschvink, J. L. & Yung, Y. L. Production of
156 hydrogen peroxide in the atmosphere of a Snowball Earth and the origin of oxygenic
157 photosynthesis. *Proc. Natl. Acad. Sci. U S A.* **103**, 18896-18899 (2006).
- 158 4 Dismukes, G. C. *et al.* The origin of atmospheric oxygen on Earth: the innovation of
159 oxygenic photosynthesis. *Proc. Natl. Acad. Sci. U S A.* **98**, 2170-2175,
160 doi:10.1073/pnas.061514798 (2001).
- 161 5 Johnson, J. E. *et al.* Manganese-oxidizing photosynthesis before the rise of cyanobacteria.
162 *Proc. Natl. Acad. Sci. USA.* **110**, 11238-11243 (2013).
- 163 6 Planavsky, N. J. *et al.* Evidence for oxygenic photosynthesis half a billion years before
164 the Great Oxidation Event. *Nature Geosci.* **7**, 283-286 (2014).
- 165 7 Crowe, S. A. *et al.* Atmospheric oxygenation three billion years ago. *Nature* **501**, 535-
166 538 (2013).
- 167 8 Havig, J. R., McCormick, M. L., Hamilton, T. L. & Kump, L. R. The behavior of
168 biologically important trace elements across the oxic/euxinic transition of meromictic
169 Fayetteville Green Lake, New York, USA. *Geochim. Cosmochim. Acta.* **165**, 389-406
170 (2015).
- 171 9 Culver, D. A. & Brunskill, G. J. Fayetteville Green Lake, New York. V. Studies of
172 primary production and zooplankton in a meromictic marl lake. *Limnol. Oceanogr.* **14**,
173 862-873, doi:10.4319/lo.1969.14.6.0862 (1969).
- 174 10 Martin, W. F., Bryant, D. A. & Beatty, T. J. A physiological perspective on the origin and
175 evolution of photosynthesis. *FEMS Microbiol. Rev.* **42**, 205-231 (2018).

- 176 11 Pavlov, A. A. & Kasting, J. F. Mass-independent fractionation of sulfur isotopes in
177 Archean sediments: Strong evidence for an anoxic Archean atmosphere. *Astrobiology* **2**,
178 27-41, doi:Doi 10.1089/153110702753621321 (2002).
- 179 12 Anbar, A. D. & Holland, H. D. The photochemistry of manganese and the origin of
180 banded iron formations. *Geochim. Cosmochim. Acta* **56**, 2595-2603 (1992).
- 181 13 Beukes, N. J. Facies relations, depositional environments and diagenesis in a major early
182 proterozoic stromatolitic carbonate platform to basinal sequence, Campbellrand
183 Subgroup, Transvaal Supergroup, Southern Africa. *Sediment Geol* **54**, 1-46 (1987).
- 184 14 Daye, M., Higgins, J., Bosak, T. Formation of ordered dolomite in anaerobic
185 photosynthetic biofilms. *Geology*. doi: <https://doi.org/10.1130/G45821.1> (2019).
- 186 15 Pibernat, I. & Abella, C. Sulfide pulsing as the controlling factor of spinae production in
187 *Chlorobium limicola* strain UdG 6038. *Arch. Microbiol.* **165**, 272-278 (1996).
- 188 16 Ha, P. T. *et al.* Syntrophic anaerobic photosynthesis via direct interspecies electron
189 transfer. *Nat Commun.* **8**, 1-7 (2017).
- 190 17 Prince, R. C. & Olson, J. M. Some thermodynamic and kinetic properties of the primary
191 photochemical reactants in a complex from a green photosynthetic bacterium. *Biochim.*
192 *Biophys. Acta-Bioenergetics* **423**, 357-362 (1976).
- 193 18 Dasgupta, J., Tyryshkin, A. M., Kozlov, Y. N., Klimov, V. V. & Dismukes, G. C.
194 Carbonate complexation of Mn²⁺ in the aqueous phase: redox behavior and ligand binding
195 modes by electrochemistry and EPR spectroscopy. *J. Phys. Chem. B.* **110**, 5099-5111
196 (2006).
- 197 19 Butterfield, C. N., Soldatova, A. V., Lee, S.-W., Spiro, T. G. & Tebo, B. M. Mn (II, III)
198 oxidation and MnO₂ mineralization by an expressed bacterial multicopper oxidase. *Proc.*
199 *Natl. Acad. Sci. USA.* **110**, 11731-11735 (2013).
- 200 20 Geszvain, K., Smesrud, L. & Tebo, B. M. Identification of a third Mn (II) oxidase
201 enzyme in *Pseudomonas putida* GB-1. *Appl. Environ. Microbiol.* **82**, 3774-3782 (2016).
- 202 21 Andeer, P. F., Learman, D. R., McIlvin, M., Dunn, J. A. & Hansel, C. M. Extracellular
203 haem peroxidases mediate Mn (II) oxidation in a marine *Roseobacter* bacterium via
204 superoxide production. *Environ. Microbiol.* **17**, 3925-3936 (2015).
- 205 22 Hemp, J. *et al.* Genomics of a phototrophic nitrite oxidizer: insights into the evolution of
206 photosynthesis and nitrification. *ISME J.* **10**, 2669-2678 (2016).
- 207 23 Hulth, S., Aller, R. C. & Gilbert, F. Coupled anoxic nitrification/manganese reduction in
208 marine sediments. *Geochimica et Cosmochimica Acta* **63**, 49-66 (1999).
- 209 24 Kurzweil, F., Wille, M., Gantert, N., Beukes, N. J. & Schoenberg, R. Manganese oxide
210 shuttling in pre-GOE oceans – evidence from molybdenum and iron isotopes. *Earth*
211 *Planet. Sci. Lett.* **452**, 69-78 (2016).
- 212 25 Ossa, F. O., Hofmann, A., Vidal, O., Kramers, J. D. & Cavalazzi, G. Unusual manganese
213 enrichment in the Mesoarchean Mozaan Group, Pongola Supergroup, South Africa.
214 *Precambrian. Res.* **281**, 414-433 (2016).
- 215 26 Beukes, N. J., Gutzmer, J. & Nel, B. Ce anomalies in similar to 2.4 Ga iron and
216 manganese formations as proxy for early oxygenation of oceanic environments. *Geochim.*
217 *Cosmochim. Acta.* **74**, A85-A85 (2010).

- 218 27 Manikyamba, C. & Naqvi, S. M. Geochemistry of Fe-Mn formations of the Archaean
219 Sandur schist belt, India - mixing of clastic and chemical processes at a shallow shelf.
220 *Precamb. Res.* **72**, 69-95 (1995).
- 221 28 Magnabosco, C., Moore, K. R., Wolfe, J. M. & Fournier, G. P. Dating phototropic
222 microbial lineages with reticulate gene histories. *Geobiology* **16**, 179-189 (2018).
- 223 29 Hazen, R. M. *et al.* Mineral evolution. *Am. Mineral.* **93**, 1693- 1720 (2008).
- 224 30 Bekker, A. *et al.* Dating the rise of atmospheric oxygen. *Nature* **427**, 117–120 (2004).

225

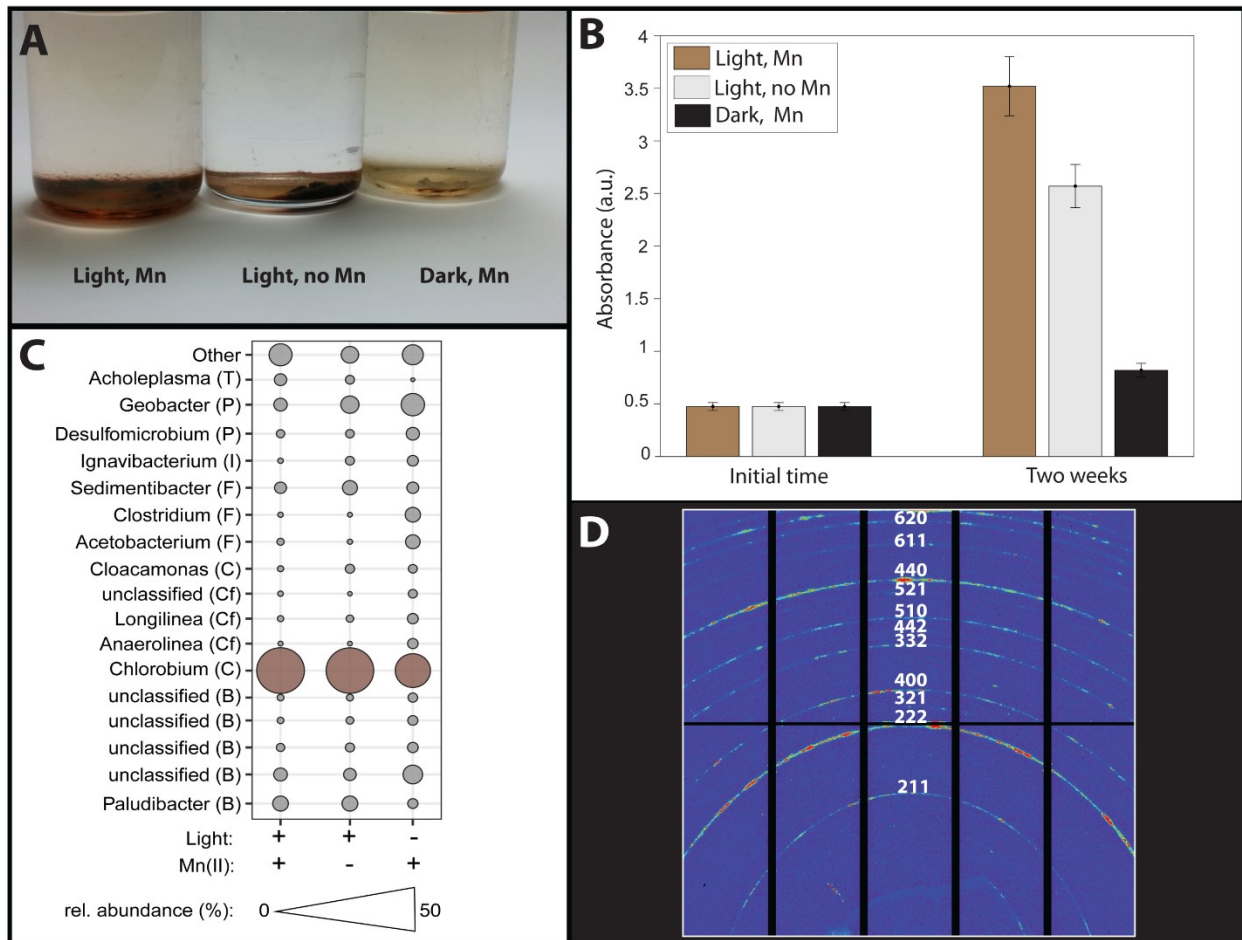
226 **Supplementary Information** is available in the online version of the paper.

227

228 **Acknowledgments:** We thank the current members of the Bosak laboratory and acknowledge
229 the support by Simons Foundation Collaboration on the Origins of Life (327126 to TB) and
230 FESD NSF project #1338810 (TB). Part of this work was performed in MIT Center for Material
231 Science and Engineering; part of Materials Research Science and Engineering Center funded by
232 National Science Foundation under award number DMR-1419807. Some analyses were carried
233 out at the Harvard University Center for Nanoscale Systems (CNS), a member of the National
234 Nanotechnology Coordinated Infrastructure Network (NNCI) supported by the National Science
235 Foundation under NSF ECCS award no. 1541959. This research used BI L12.3.2, a resource of
236 the Advanced Light Source, which is a DOE Office of Science User Facility under contract no.
237 DE-AC02-05CH11231. MP received funding from John Templeton foundation and the Professor
238 Amar G. Bose Research Grant Program, MIT.

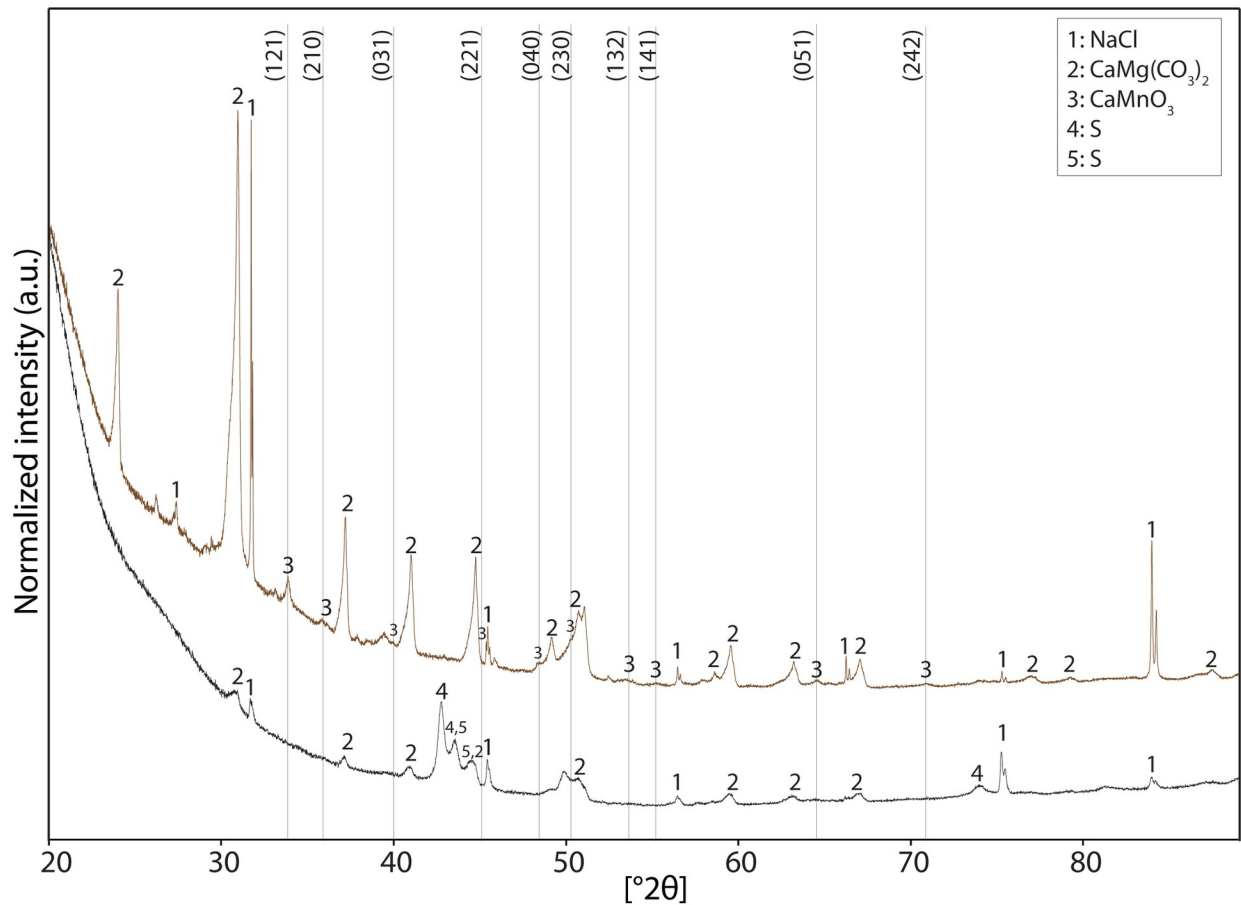
239 **Author Contributions** M.D. and T.B. conceived and designed the project, conducted pilot
240 studies and collected preliminary data. M.D., S.R., N.T and M.P. performed the experiments.
241 V.K.-C, A.F.-R. and S.R. analyzed microbial communities and performed bioinformatic
242 analyses. M.D and T.B wrote the manuscript with input from M.P. and V.K.-C., and N.B. All co-
243 authors reviewed and approved the final manuscript.

244



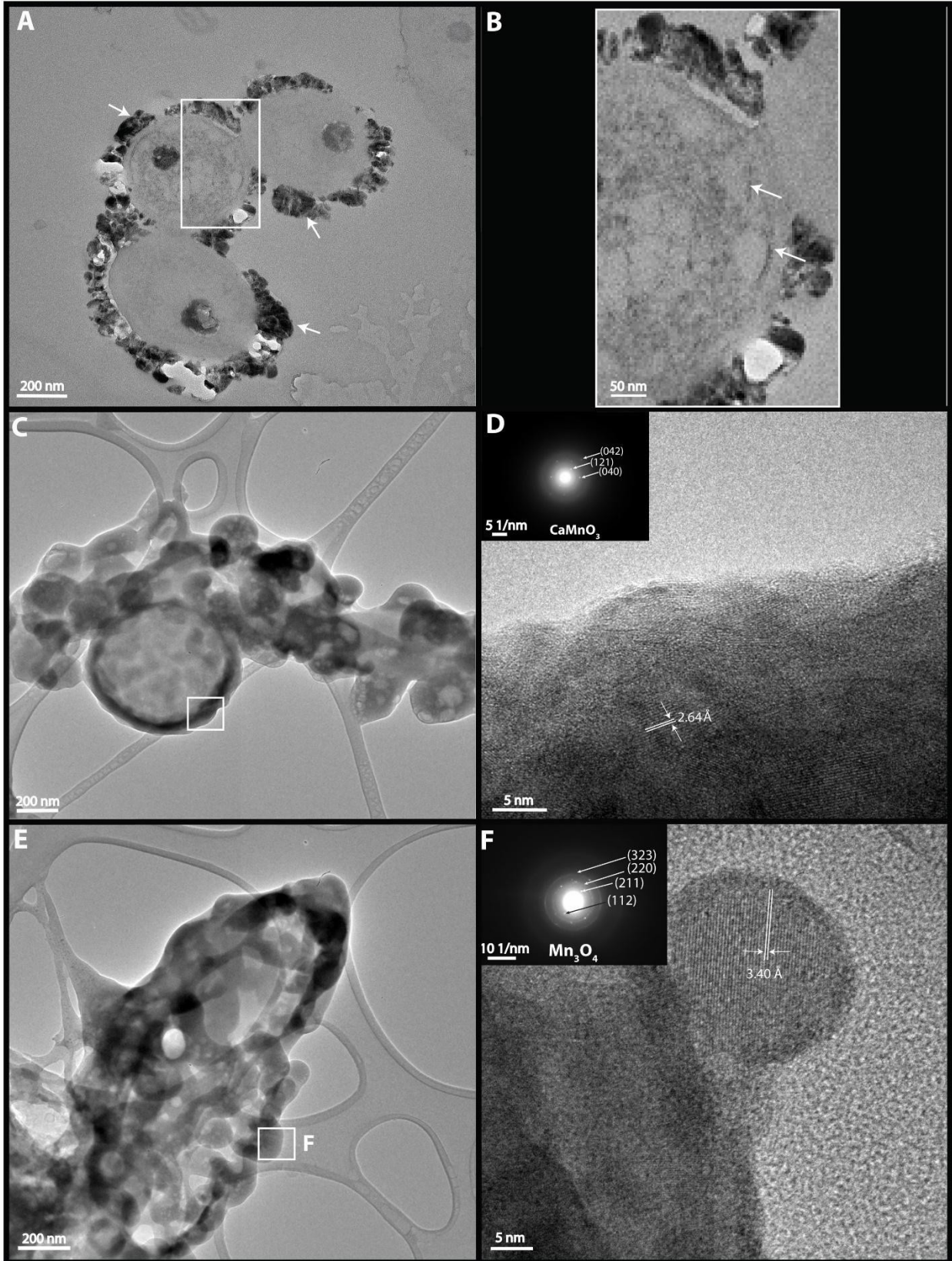
245
247 **Figure 1.** Biofilms incubated for two weeks. A: Dark brown biofilm incubated in the light with
248 Mn(II) covers the entire bottom of the culture bottle. Biofilm incubated in the light without
249 Mn(II) covers only a portion of the bottom. Biofilm incubated in the dark with Mn(II) is yellow.
250 B: Biomass of biofilms measured by the crystal violet assay. All incubations were performed in
251 triplicate. C: Microbial diversity in biofilms obtained by high-throughput Illumina sequencing of
252 16S rRNA genes. The most abundant taxon across all conditions was a *Chlorobium* sp. (30-
253 60%). This microbe was more abundant in photosynthesizing cultures (Extended Data). D:
254 Diffraction pattern indexes for Mn_3O_4 in the spectrum acquired by synchrotron micro-focused X-
255 ray diffraction (μ XRD) of a biofilm incubated in the light for two weeks.

256
257



258
 259 **Figure 2.** X-ray diffraction spectra (XRD) of biofilms incubated for two weeks. Top spectrum:
 260 biofilms incubated in the light with 1 mM Mn(II). Black lines indicate Miller indices (*hkl*)
 261 assigned to each peak of CaMnO₃. Bottom spectrum: biofilms incubated in the dark with 1 mM
 262 Mn(II). Biofilm incubated in the dark contains sulfur phases (S, “4” and “5”) that formed during
 263 the treatment to remove oxidized manganese minerals before inoculation (see Methods 1.1.1.,
 264 Extended Data Fig. 10 and Methods 3.2 for the interpretation of XRD peaks).

265
 266
 267



270 **Figure 3.** Microbe-mineral interactions in biofilms incubated with Mn(II) in the light for two
271 weeks. A: Mineral-encrusted cells (white arrows) in fixed and stained samples (TEM at 80 kV);
272 white square indicates the area magnified in panel B. B: Chlorosomes (white arrows) in a cell
273 that is encrusted by manganese oxide precipitates (TEM at 80 kV, fixed and stained sample). C:
274 TEM at 200 kV of unprocessed and unstained microbial cells. Minerals encrust the cell envelope.
275 White squares indicate the regions selected for SAED shown in panel D. D: High resolution
276 TEM and selected area electron diffraction (SAED) of minerals around an unstained cell from a
277 fresh suspension of the microbial culture on a TEM grid. The indexes of the SAED pattern
278 correspond to CaMnO_3 with the d-spacing of 2.64 Å. E: TEM at 200 kV of unprocessed and
279 unstained microbial cells. Minerals encrust the surface of the cell. White square indicates the
280 region selected for SAED shown in panels F. F: HRTEM and SAED of minerals in the area
281 outlined by the white square in E. The indexes of the SAED pattern correspond to Mn_3O_4 with d-
282 spacing of 3.40 Å.
283
284
285
286
287

288 **METHODS**

289 **1. Culturing and sequencing**

290 **1.1. Enrichment and culturing conditions**

291 Sediments were retrieved from Fayetteville Green Lake (FGL) by a metallic gravity scoop and
292 stored at 4°C in fully filled, hermetically sealed glass jars. These samples were used as inoculum
293 for enrichment cultures in the FGL medium described below. All inoculations were conducted in
294 an anaerobic chamber under a 5%CO₂: 5%H₂: balN₂ (v/v/v) atmosphere using standard anaerobic
295 techniques³¹. Briefly, FGL medium was flushed before and after autoclaving in hermetically
296 sealed glass bottles. Sterile flushed FGL medium was inoculated inside the anaerobic chamber
297 (5% H₂/15% CO₂/80% N₂ atmosphere). To avoid any issues associated with the exposure of
298 biofilms to H₂, the serum bottles were opened inside the anaerobic chamber, inoculated in about
299 1 minute, closed immediately, capped and flushed again with CO₂/N₂ for 60-75 minutes to
300 remove H₂. All experiments were conducted in batch cultures and all cultures were inoculated by
301 approximately 1 mg of biofilm that had been washed six times by anoxic nanopure water^{32,33},
302 mechanically dispersed by passing through a syringe and resuspended in sterile anaerobic
303 medium. All these steps were carried out in the anaerobic glove box. All enrichment cultures
304 were incubated at 27°C with incandescent white light bulb and a 12:12h day/night cycle. All
305 enrichment cultures were incubated at 27°C with incandescent white light bulb and a 12:12h day/
306 night cycle. All plasticware used in the anaerobic chamber was introduced into the chamber at
307 least one week before the experiments.

308 The culture medium (FGL medium) contained: 0.1 mM KH₂PO₄, 5.61 mM NH₄Cl, 0.9
309 mM KCl, 0.024 M NaHCO₃, 1 mM MnCl₂.2 H₂O, 1 mM Na₂SO₄, 1 ml/L of trace element
310 solution. The trace element solution was prepared in 10% (v/v) HCl and contained per liter; 1.5
311 g FeCl₂.4H₂O, 190 mg CoCl₂.6H₂O, 100 mg MnCl₂.4H₂O, 70 mg ZnCl₂, 31 mg Na₂MoO₄, 6 mg
312 H₃BO₃, 2 mg CuCl₂.2H₂O. The pH of the medium was adjusted to 7 by the addition of NaOH
313 (1M) or HCl (1 M). After adjusting the pH to 7, the FGL medium was distributed into glass
314 bottles of different volumes (12, 25, 50, 150, 200 mL). The final background concentration of
315 manganese was 0.4 µM. To inhibit the growth of oxygenic phototrophs, we added 0.01 mM
316 DCMU (3-(3,4-dichlorophenyl)-1,1-dimethylurea) to the initial enrichments. All analyses
317 described in the main text used later enrichments that were grown in DCMU-less media. Glass
318 serum bottles were capped by butyl rubber stoppers and aluminum seals. Before autoclaving, the
319 FGL medium in bottles were flushed by 20% CO₂: 80% N₂ for one hour, the serum bottle
320 headspaces for another 40 minutes total. The bottles were then autoclaved (40 minutes sterile).
321 After autoclaving, the FGL medium in bottles were flushed again by 20% CO₂: 80% N₂ for one
322 hour, the serum bottle headspaces for another 40 minutes total after cooling.

323 A separately prepared selenium stock solution contained 2 mg of Na₂SeO₃ in 1000 mL of
324 0.01 M NaOH. This solution was autoclaved and made anaerobic by flushing the bottles for 1 hr
325 and 40 min with 20% CO₂: 80% N₂. The vitamin solution was prepared in nanopure water by
326 aerobic filter sterilization and contained per liter: 2 mg biotin, 2 mg folic acid, 10 mg pyridoxine-
327 2H₂O, 5 mg thiamine-HCl-2H₂O, 5 mg riboflavin, 5 mg nicotinic acid, 5 mg D-Ca-pantothenate,
328 0.1 mg vitamin B12, 5 mg p-aminobenzoic acid, 5 mg lipoic acid.

329 The master stock solution (20x) contained 1.5 mM MgCl₂.6H₂O, 1 mM CaCl₂.2 H₂O, 1
330 mL of vitamin solution and 1 ml of the selenium stock solution in 50 mL nanopure water. The
331 master solution was filter-sterilized and flushed for 1 hr and 40 min by 20% CO₂: 80% N₂ gas

332 mixture. This solution was added to the FGL medium immediately before inoculation, 5 mL per
333 100 ml medium. Manganese was added at the time of inoculation from concentrated anaerobic
334 stock solution of $\text{MnCl}_2 \cdot 4\text{H}_2\text{O}$ (1 M). Finally, after inoculation, the medium was reduced by the
335 addition of sulfide from a concentrated anaerobic stock solution of $\text{Na}_2\text{S} \cdot 5\text{H}_2\text{O}$ (0.2 M).

336 The medium used for the initial enrichment was reduced by the addition of 4 mM sodium
337 ascorbate instead of sulfide to minimize the growth of organisms that require high concentrations
338 of sulfide as an electron donor. A brown microbial mat formed on the surface of the inoculated
339 sediments after 3-4 weeks. Fragments of this mat were transferred into the sterile medium with
340 the same composition as described above, incubated in the same conditions for one month, and
341 transferred again. All experiments described here used biofilms that had undergone at least four
342 transfers from the initial enrichment.

343

344 **1.1.1. Modified FGL medium.** All experiments described in the main text used the modified
345 basal FGL (MFGL) medium. This medium did not contain DCMU, sulfate or ascorbate, and was
346 reduced by 20-50 μM Na_2S . Sterile MFGL contained only traces of sulfate ($< 0.9 \mu\text{M}$), nitrate ($<$
347 $0.5 \mu\text{M}$) and nitrite ($< 0.1 \mu\text{M}$), as detected by ion chromatography (see section 5).

348 To evaluate the influence of light on growth, biofilms from the third transfer were
349 inoculated into the MFGL medium. One triplicate set of batch cultures was incubated for two
350 weeks in the light at 27°C at a distance of 35 cm from an incandescent white light bulb that emits
351 between 400-700 nm. Another set was incubated at the same time and at the same temperature
352 but was shielded from the light by aluminum foil.

353 To reduce the carryover of manganese oxides in the biofilm inoculum, we reduced the
354 inoculums using a previously described protocol³⁴. Briefly, microbial biofilms that had been
355 grown in the presence of light and 1 mM Mn(II) were harvested and incubated in anaerobic
356 sterile ascorbic acid (0.25 mM) in the anaerobic chamber for 10 minutes. After this incubation,
357 the biofilms were washed three times with sterile, anaerobic nanopure water. XRD analyses of
358 biofilms treated in this manner showed that this protocol removed manganese oxide minerals but
359 increased the abundance of elemental sulfur in the inoculum (Extended Data Fig. 10). Elemental
360 sulfur was absent from the biofilms before the treatment (Fig. 2a).

361 To characterize the effect of different initial concentrations of manganese and sulfide on
362 mineral precipitation, biofilms from the third transfer of the original enrichment culture were
363 inoculated into the MFGL medium amended by MnCl_2 , and Na_2S from 0.5 M and 0.1 M
364 anaerobic stock solutions. All stock solutions were prepared, autoclaved and stored under an
365 atmosphere of N_2 . The effect of Mn concentration on manganese oxidation was evaluated in three
366 sets of triplicate inoculated cultures that contained 0.1, 1 or 5 mM MnCl_2 . All these cultures were
367 reduced with 50 μM Na_2S . The effect of H_2S concentration on manganese oxidation was explored
368 in three sets of triplicate cultures reduced by 0.05, 0.25 or 1 mM of Na_2S , all amended with 1
369 mM MnCl_2 . An additional set of triplicate cultures contained 1 mM Mn(II) and 0.02 mM Na_2S .
370 All cultures were incubated for two weeks.

371

372 **1.2. Further enrichment of Mn-oxidizing and sulfide-oxidizing microbes**

373 Microbial communities capable of anaerobic oxidation of manganese were further enriched by
374 inoculating anaerobically sealed agar shake tubes with the dispersed biofilms, serially diluting
375 the cultures in agar, transferring colonies into liquid medium and repeating the entire process for

376 the second time^{35,36}. The MFGL medium in agar shake tubes was solidified by 1.1 % agar.
377 Biofilms were washed with anaerobic nanopure water in the anaerobic glove box and
378 mechanically dispersed in 10 ml of the basal MFGL medium. The first agar shake tube was
379 inoculated with 10% (1 ml) of the dispersed inoculum and diluted by five successive transfers of
380 1 ml into 9 ml of sterile MFGL.

381 The additions of sulfide and manganese to the basal MFGL in agar shake tubes targeted
382 two different conditions: Condition 1) 0.02 mM Na₂S and 1 mM MnCl₂ sought to enrich for
383 microbes that can photosynthesize in the presence of low sulfide concentrations and oxidize
384 Mn(II); Condition 2) 1 mM Na₂S (MnCl₂ added only in the trace metal solution) enriched for
385 *Chlorobium spp.* that can oxidize sulfide. Extended Data Table 2 summarizes the enrichment
386 protocol and conditions. The shake tubes were incubated at 27°C at a distance of 35 cm from the
387 incandescent white light bulb. Colonies that formed after one month were transferred from the
388 solid medium into the liquid medium that contained the same concentrations of MnCl₂ and Na₂S.
389 Biofilms that grew in liquid after one month were mechanically dispersed by a syringe,
390 inoculated into another set of agar shake tubes and incubated for one month. Colonies from the
391 shake tubes were inoculated again into the liquid medium. The purity of the cultures at each
392 transfer was tested by Sanger sequencing. Amplified 16S rRNA genes were sequenced in both
393 directions using either 27F (5'-AGAGTTTGATCCTGGCTCAG-3') or 1492R (5'-ACG GCT
394 ACC TTG TTA CGA CTT-3') (IDT Integrated DNA Technologies, Inc., Coralville, IA, USA),
395 assembled to get a nearly full-length 16S rRNA gene (GeneWiz, Madison, WI, USA) and
396 identified using nucleotide BLAST on GeneBank³⁷. Future experiments should also explore the
397 possibility of light-dependent production of organoperoxides in the medium as a function of
398 vitamins and Fe(II) in the medium.

399

400 **1.3. DNA extraction, 16S rRNA gene Illumina sequencing and phylogenetic analyses**

401 A 500 µl sample of each biofilm enrichment (including early enrichments and the lake inoculum)
402 was harvested and spun down into a pellet. Total DNA was extracted from samples using the
403 PowerSoil® DNA Isolation Kit (MoBio, Carlsbad, CA, USA) according to manufacturer's
404 instructions and eluted in 60 µl C6 solution. Upon extraction, DNA was quantified using
405 NanoDrop (Thermo Scientific, Inc., Wilmington, DE, USA). The extracted samples and blank-
406 template controls from the PowerSoil DNA Isolation kit were stored at -80°C and sent to
407 Argonne National Lab (Lemont, IL, USA) on dry ice for sequencing. The community
408 composition was characterized using 16S rRNA gene amplicon paired-end sequencing on the
409 MiSeq Illumina platform. Briefly, V4 region of the 16S rRNA gene (515F-806R) from each
410 sample was amplified using the bacterial-specific primers 515F (5'-
411 GTGCCAGCMGCCGCGGTAA-3') and 806 R (5'-GGACTACHVGGGTWTCTAAT-3') using
412 PCR conditions³⁸. After the amplifications, the PCR amplicons were quantified using Quant-iT
413 PicoGreen dsDNA Assay Kit (ThermoFisher/ Invitrogen cat. no. P11496) according to
414 manufacturer's instructions and pooled in equal concentrations (240 ng) to a single tube. This
415 pool was cleaned up using MoBio UltraClean PCR Clean-Up Kit (MoBio, Carlsbad, CA, USA)
416 and quantified using the Qubit (Invitrogen, Carlsbad, CA, USA). The pooled samples were
417 sequenced on the Illumina MiSeq platform (Illumina, San Diego, CA, USA). All library
418 preparations, pooling, quality controls and sequencing runs were performed at the Argonne
419 National Lab (Lemont, IL, USA). Sequence data were analyzed using QIIME v.1.9.0³⁹. Paired-
420 end reads were joined using fastq-join method⁴⁰, and libraries were demultiplexed and filtered.

421 Any reads that did not assemble by perfect matches in the overlapping region or meet the q-score
422 (>20) threshold were removed and were not used in subsequent analyses. Chimeric sequences
423 were identified using UCHIME's usearch61 *de novo* based chimera detection algorithm⁴¹ and
424 removed from the quality-filtered sequences. Filtered and chimera-free sequences were aligned
425 and clustered into operational taxonomic units (OTUs) at >97% similarity level using closed-
426 reference UCLUST algorithm against the Greengenes v13.8 reference dataset as a database⁴².
427 The most abundant sequence from each cluster was selected as a representative sequence. All
428 representative sequences were aligned using PyNAST³⁹. A phylogenetic tree for subsequent
429 phylogenetic analyses was built using FastTree⁴³. OTU counts were rarified to 10,000 sequences
430 per sample for diversity analysis using taxonomic and phylogenetic indices that included the
431 Shannon and Faith's PD index. To identify bacterial taxa whose sequences are more abundant in
432 samples grown in light and/or with Mn(II), we used LEfSe which performs a nonparametric
433 Wilcoxon sum-rank test followed by linear discriminant analysis (LDA) coupled with effect size
434 measurements to assess differentially abundant taxa⁴⁴. *Chlorobium* sequences were significantly
435 enriched in samples grown in the presence of light and Mn(II) with LDA score >5. Cultures
436 grown in light had significantly more *Chlorobium* sp. (ANOVA, F = 23.4521, df factor = 5, df
437 error = 12, p < 0.0001; Tukey's HSD, p < 0.01). Sequence data are available as FASTQ files at
438 the National Center for Biotechnology Information (NCBI) via Sequence Read Archive (SRA),
439 under the SRA accession ID number SRP133329.

440

441 **1.4. Metagenome sequencing and analysis**

442 To determine the metabolic potential of cultures grown from colonies that targeted specific
443 growth conditions (see Section 1.2), we sequenced their metagenomes. The DNA of enrichments
444 obtained using Condition 1 was extracted using a modified phenol-chloroform method with
445 ethanol precipitation previously described⁴⁵ and quantified by a Qubit 2.0 Fluorometer (Thermo
446 Fisher Scientific, Chino, CA, USA). This DNA was sent for metagenomic sequencing to the
447 University of Southern California's Genome and Cytometry Core Facility (Los Angeles, CA,
448 USA). The library preparation, quality control, and sequencing were performed at the Cytometry
449 Core Facility. Briefly, before sequencing on Illumina HiSeq 2500 platform, DNA was sheared
450 using dsDNA Shearas Plus (Zymo, Irvine, CA, USA), cleaned up using Agencourt AMPure XP
451 beads (Beckman-Coulter, Indianapolis, IN, USA), the library was quantified using the Qubit 2.0
452 Fluorometer and the DNA fragment size was determined with an Agilent Bioanalyzer 2100.

453 The quality control of the sequence data was performed using Trimmomatic v0.36 using
454 default parameters and a minimum sequence length of 36 bp⁴⁶. IDBA-UD v1.1.2. was used to
455 assemble the reads with a 2000 bp minimum contig length. SAMtools v.1.3.1⁴⁷ was used to
456 convert files to binary format for downstream analysis. VizBin was used to delineate individual
457 genomes from the enrichment metadata⁴⁸ and the genomes were assigned putative taxonomic
458 identities according to their placement in a phylogenetic tree in CheckM v.1.0.4 using the "tree"
459 command⁴⁹.

460 Individual genomes obtained from the metagenome data were submitted to the DOE Joint
461 Genome IMG-MER (Integrated Microbial Genomes) pipeline for gene calling and assembly⁵⁰.
462 Protein-coding gene-prediction tool Prodigal v.3.0.0 was used to determine genes in the
463 enrichment grown from the colony on 1 mM MnCl₂ and 20-50 μM Na₂S. The genome of *C.*
464 *limicola* was 98.4% similar to *Chlorobium limicola* Frassasi⁵¹.

465 To detect putative Mn(II)-oxidizing genes in *Chlorobium limicola*, we first generated a
466 blast database of protein-coding Mn(II)-oxidizing genes by selecting genes encoding for multi-
467 copper oxidases (MCOs) and animal heme peroxidases (AHPs). Because MCOs and AHPs each
468 contain several classes of enzymes and can transfer electrons from a number of different
469 substrates, we focused on enzymes with confirmed manganese-oxidizing activities by
470 biochemical and molecular assays. All MCOs and AHPs involved in Mn(II)-oxidation and
471 characterized to date are from aerobic microorganisms and include genes such as *mnxG*, *mcoA*,
472 and *mopA* in *Pseudomonas putida*¹⁹, *mnxG* in the spores of *Bacillus* strain SG-1¹⁸, *moxA* in
473 *Pedomicrobium* sp. ACM 3067⁵², *mopA* in *Aurantimonas manganoxydans* SI85-9A1⁵³, and
474 *Roseobacter* sp. AzwK-3b²⁰. To determine whether *Chlorobium* has any homologs with
475 characterized manganese-oxidizing MCOs and AHPs, we used BLASTp⁵⁴ and queried translated
476 Mn(II)-oxidizing genes against the *Chlorobium* genome with an e-value cutoff of 10⁻⁵ and a bit
477 score of 30. Homologs of MCOs and AFPs in *C. limicola* are shown in Extended Data Table 4.

478 Sequence data for *C. limicola* can be accessed at the JGI-IMG under IMG Submission ID
479 124328.

480

481 2. Spectroscopy

482 2.1. X-ray photoelectron spectroscopy

483 X-ray photoelectron spectroscopy was performed on a K-alphaTM + X-ray photoelectron
484 spectrometer (XPS, K-Alpha + XPS, Thermo Fisher, MA, USA). Biofilms were harvested and
485 centrifuged at 14,000 rpm for 5 min in the anaerobic chamber to form pellets. The pellets were
486 placed on double-sided carbon tape and dried in the anaerobic chamber. To maintain the anoxic
487 conditions, the samples were stored in the anaerobic chamber in hermetically sealed glass vials
488 before analysis. All samples were fractured in high vacuum (3×10⁻⁸ Torr) in the Kratos outer
489 pressure chamber and then moved directly into the main XPS measurement chamber. An
490 incident monochromatic X-ray beam from the Al K Alpha target (15 kV, 10 mA) was focused on
491 a 0.4 mm × 0.3 mm area of the surface at a 45° angle with respect to the sample surface. Depth
492 profile etching with an etch cycle of 30 s and a total of 10 levels yielded high resolution spectra.
493 The electron energy analyzer perpendicular to the sample surface was operated with a pass
494 energy of 50 eV to obtain XPS spectra at a 0.1 eV step size and a dwell time of 50 ms. Each peak
495 was scanned 15 times. To ensure representative data from heterogeneous samples, we probed a
496 total of 50-80 points per sample. XPS data were treated and analyzed using CasaXPS curve
497 resolution software package. Spectra were best fit after Shirley background subtractions by non-
498 linear least squares CasaXPS curve resolution software package. Gaussian/Lorentzian (G/L)
499 contributions to the line shapes were numerically convoluted using a Voigt function. The
500 different XPS lines with sets of Gaussian and Lorentzian peaks were empirically fitted with
501 different standards corresponding to different oxidation sets (MnO, MnCO₃, Mn₂O₃, Mn₃O₄,
502 MnO₂, MnCaO₃). Each Mn XPS spectrum was empirically best fitted with multiple standard
503 phases (MnO, MnCO₃, Mn₂O₃, Mn₄O₃, MnO₂, MnCaO₃) that produced the minimum residual.
504 The average fit properties for all treated spectra were acceptable as the following: R expected=
505 1.60, R profile= 1.71, significance level= 0.05, residual standard deviation= 1.67, goodness of
506 fit= 1.78, critical Chi-square= 3.84.

507

508 2.2. Interpretation of XPS spectra

509 The redox state of manganese in microbial cultures was confirmed by XPS (Extended Data Fig.
510 3). The Mn2p XPS spectra of the dark culture exhibited two major peaks at binding energies of
511 640.90 eV and 652.2 eV corresponding to Mn2p_{2/3} and Mn2p_{1/2}, respectively. This is in agreement
512 with other reports on Mn(II) phases of Mn^{55,56}. In the photosynthesizing culture, the Mn2p peak
513 shifted to a high-energy side and the intense satellite peak characteristic of Mn(II) diminished.
514 These biofilms contained Mn in different valence states. At some analyzed spots, the Mn2p XPS
515 spectrum exhibited two major peaks of Mn2p_{2/3} and Mn2p_{1/2} at binding energies of 642 eV and
516 653 eV, respectively. These correspond to Mn(IV) in calcium-manganese oxide phases⁵⁷. Peaks
517 at Mn2p_{2/3} with binding energies 641.61 eV and 641.47 eV, respectively, were also detected.
518 These peaks correspond to Mn(III) in Mn₂O₃ and Mn(III) and Mn(II) in Mn₃O₄ phases^{58,59}.

519 The redox state of the manganese in the culture enriched in condition 1 and condition 2
520 was confirmed by XPS (Extended Data Fig. 8). The Mn2p XPS spectra of this culture (Extended
521 Data Fig. 8a) exhibited two major peaks at binding energies of 641.41 eV and 653.15 eV
522 corresponding to Mn2p_{2/3} and Mn2p_{1/2}, respectively and matching Mn₃O₄⁵⁸. The Mn2p XPS
523 spectra of Condition 2 enrichment (Extended Data Fig. 8b) exhibited Mn2p_{2/3} peaks at 640.97 eV
524 and 652.2 eV corresponding to Mn2p_{2/3} and Mn2p_{1/2} respectively. This is in agreement with other
525 reports of MnO phase⁶⁰.

526

527 **2.3. Probing the redox state of manganese in biofilms**

528 We used X-ray Photoelectron Spectroscopy (XPS) to detect oxidized manganese in colonies
529 enriched on 1 mM Mn(II) (Condition 1). Table 3 in Extended Data summarizes the procedure
530 used to study the Mn(II) oxidation activity in the enrichment cultures. Manganese oxidation was
531 tested using cultures that were enriched as colonies in agar shake tubes (Condition 1, Condition
532 2, Section 2, Table 3 in Extended Data). Biofilms from condition 1 were grown in duplicate 10
533 ml cultures with 1 mM MnCl₂ and 0.02 mM Na₂S, mechanically dispersed and resuspended into
534 separate 10 ml liquid solutions. Five percent v/v of this suspension was transferred into 10 ml of
535 MFGL medium with 1 mM MnCl₂ and 0.02 mM Na₂S and the cultures were incubated at 27 °C
536 for one week before the assay. A second assay tested the Mn(II) oxidation activity without
537 requiring the very sparse biofilm to grow. Condition 1 enrichment was grown for two weeks as
538 described above, centrifuged at 8000 rpm in the anaerobic chamber, washed 3 times with
539 anaerobic water and transferred into 10 ml of MFGL with 1 mM MnCl₂ and 0.02 mM Na₂S.
540 These cultures were incubated for 3 days in a 12 h/12 h light/dark regime and harvested
541 anaerobically. This procedure preserved the cell density of the original biofilms and did not
542 require microbial growth.

543 To test for Mn (II) oxidizing activity in the enrichment from condition 2 (*Chlorobium* sp.
544 and *Desulfomicrobium* sp.), the culture was grown in 10 ml of the basal MFGL amended with 1
545 mM Na₂S, harvested anaerobically, and dispersed in 10 ml of the basal MFGL medium. This
546 suspension was used to inoculate 10 ml of the basal MFGL amended with 1 mM MnCl₂ and 0.02
547 mM Na₂S at 5% v/v. The inoculated medium was incubated in the light/dark regime for one
548 week. To test for Mn(II) oxidizing activity without requiring the low-biomass biofilms to grow,
549 the enrichment from condition 2 was grown for two weeks in 10 ml of the basal MFGL amended
550 with 1 mM Na₂S, centrifuged at 8000 rpm in the anaerobic chamber, washed 3 times with
551 anaerobic water and transferred to 10 ml of MFGL with 1 mM MnCl₂ and 0.02 mM Na₂S. These
552 cultures were incubated for three days in the 12h/12h light/dark regime and harvested
553 anaerobically. All collected microbial pellets were dried on carbon tape and stored anaerobically

554 inside serum bottles with N₂ atmosphere and placed inside the anaerobic chamber in the dark at
555 26 °C until XPS analysis.

556

557 **2.3.1. Probing the redox state of manganese in co-cultures**

558 *Chlorobium limicola* (DSM 245, DSMZ GmbH Germany) and *Chlorobium tepidum* (DSM
559 12025, DSMZ GmbH, Germany) were inoculated with 5% v/v inoculum and grown in 50 ml
560 MFGL medium supplemented with 0.05 mM Na₂S and 0.5 g/L yeast extract in a 12 h/12 h light/
561 dark regime at 27 °C for 3 weeks. *Geobacter lovleyi* (DSM 17278, DSMZ GmbH Germany) was
562 grown in MFGL supplemented with 2.8 mM ferrihydrite and 5 mM acetate and reduced with
563 0.05 mM Na₂S in the dark at 21 °C for 3 weeks. Microbes from these cultures were inoculated as
564 5% v/v inoculum in the following combinations: *C. limicola* + *C. tepidum*, *C. tepidum* + *G.*
565 *lovleyi*, *C. limicola* + *G. lovleyi*, *C. limicola* + *C. tepidum* + *G. lovleyi*. All these co-cultures
566 were grown in 10 ml MFGL medium with 1 mM Mn(II) and 0.05 mM Na₂S in a 12 h/12 h light/
567 dark regime at 27 °C for 2 weeks. The biomass was harvested anaerobically, the pellets were
568 dried on carbon tape and stored anaerobically under N₂ inside the anaerobic chamber in the dark
569 at 26 °C until XPS analysis. The oxidation state of Mn was characterized by XPS in all four
570 cultures.

571

572 **3. X-ray powder diffraction**

573 X-ray powder diffraction (XRD) patterns were obtained in reflection mode with Ni-filtered Cu
574 K α radiation ($\lambda = 1.5406 \text{ \AA}$) as X-ray source on an X'Pert PRO diffractometer (XRD, X'Pert
575 PRO, PANalytical, Netherlands) equipped with an X'Celerator detector (PANalytical,
576 Netherlands). The patterns were measured in 2Θ range from 3° to 90° with a scanning step of
577 0.008° and a fixed counting time of 600 s at 45 kV and 40 mA. Biofilms were harvested and
578 centrifuged at 14,000 rpm for 5 min in the anaerobic chamber. Microbial paste was smeared on
579 Zero Diffraction Disk (23.6 mm diameter x 2.0 mm thickness, Si crystal, MTI corporation, CA,
580 USA) and dried in the anaerobic chamber. The samples were analyzed inside the anaerobic dome
581 to maintain the anoxic conditions during the XRD analyses. Data were analyzed and fitted using
582 High Score Plus program version 4.5. The average fit properties for all treated spectra were
583 acceptable as the following: Residual Standard Deviation= 1.63, R expected= 1.28, R profile=
584 1.63, Significance level= 0.05, Goodness of Fit = 1.69, Critical Chi-square = 3.84.

585 Precipitated minerals were also analyzed using in-situ synchrotron-based X-ray
586 diffraction (SR-XRD) at the Advanced Light Source (ALS) at the beamline 12.3.2. Biofilms were
587 harvested on site and the biofilm paste was loaded into transmission sample XRD cells. The
588 transmission synchrotron diffraction data were collected using a DECTRIS Pilatus 1M hybrid
589 pixel area detector placed at an angle 2Θ of 35° at approximately 170 mm from the sample. The
590 4-bounce monochromator was set to an energy was 10 keV ($\lambda = 1.239842 \text{ \AA}$). The sample
591 geometry with respect to the incident beam and the detector was carefully calibrated using Al₂O₃
592 powder. The 2D diffraction patterns (Fig.1d) were analyzed and integrated along the azimuthal
593 direction into 1D diffractograms using the X-ray microdiffraction analysis software (XMAS v6)
594 developed at the Advanced Light Source for the ALS beamline 12.3.2 and Matlab R2017a.

595

596 **3.1. Determination of XRD detection limit**

597 To determine the detection limit of XRD, 0.05, 0.01, 0.02, and 1 mg of MnO₂ was mixed with 10
598 mg of dry anaerobic biofilm that did not contain green sulfur bacteria or manganese oxides and
599 spread on Zero Diffraction Disk (23.6 mm diameter x 2.0 mm thickness, Si crystal, MTI
600 corporation, CA, USA). The mixtures were analyzed by X'Pert PRO diffractometer XRD, X'Pert
601 PRO, PANalytical, Netherlands) equipped with an X'Celerator detector (PANalytical,
602 Netherlands) over 10-hour analysis time. MnO₂ standard and the bacterial biofilm were also run
603 separately as controls. The detection limit of XRD was determined by the mass of MnO₂ that
604 yielded discernible diffraction peaks in the XRD spectrum.

605

606 **3.2. Interpretation of XRD peaks**

607 The XRD spectra of microbial cultures incubated in the light with Mn(II) (Fig. 2) showed peaks
608 that can be indexed to a ternary manganese oxide; CaMnO₃ (ICDD-01-016-2217) with lattice
609 constants of a= 5.2917 nm, b= 7.4803 nm and c= 5.2870 nm⁶¹. CaMnO₃ is not known to occur
610 naturally.

611 Dolomite was the most abundant phase in the cultures and its peaks were indexed as
612 (104), (101), (110), (11-3), (202) and (018) (ICDD-04-011-9833). The absence of light inhibited
613 the growth of photosynthetic microbes and the formation of manganese oxide minerals and also
614 reduced the precipitation of dolomite (Fig. 2). Biofilm incubated in the dark showed the
615 precipitation of calcium carbonate phase, CaCO₃ (ICDD-00-058-0471) indexed for (121) and
616 (102). In addition to the various carbonate phases, the XRD spectrum showed two different
617 phases of sulfur (S⁰); (ICDD-04-020-2294) indexed for (110), (-101) and (-211) and (ICDD-05-
618 001-0219) indexed for (110) and (-101).

619 The XRD spectra of microbial cultures incubated at different concentrations of Mn and S
620 showed peaks of manganese oxide, dolomite and elemental sulfur (Extended Data Fig. 5). The
621 latter formed in microbial cultures incubated at high concentrations of H₂S (0.25-1 mM) and in
622 the cultures grown with less than 1 μM Mn(II) (Extended Data Fig. 6; see trace metal solution
623 composition in Section 1.1.). Elemental sulfur, S⁰ (ICDD-05-001-0219), was indexed for (110),
624 (-101), (011) and (-211).

625 Extended data Fig. 10 shows two XRD spectra of microbial cultures incubated in the
626 light. The top spectrum is the analysis of microbial biofilms without treatment showing peaks of
627 manganese oxide, CaMnO₃ (ICDD-01-016-2217) and dolomite, CaMg(CO₃)₂ (ICDD-04-011-
628 9833). The bottom spectrum is the analysis of treated microbial biofilms showing only peaks of
629 elemental sulfur S⁰ (ICDD-05-001-0219) and a calcium carbonate phase, CaCO₃ (ICDD-00-058-
630 0471).

631

632 **4. Microscopy**

633 **4.1. Scanning electron microscopy**

634 Scanning electron micrographs were acquired by a Zeiss Merlin scanning electron microscope
635 with the GEMINI II column (SEM, Zeiss Merlin SEM, Carl Zeiss microscopy, CA, USA). The
636 microscope was equipped with a field gun emission and energy dispersive X-ray spectrometer
637 (EDS, EDAX detector; EDAX, NJ, USA) that operated at an accelerating voltage of 5 - 15 kV,
638 probe current of 100 pA, and a working distance of 8.5 mm. On-axis in-lens secondary electron
639 (SE-mode) detector was used during imaging. The samples were fixed by 0.2 M sodium
640 cacodylate, 0.1% CaCl₂ and 2.5% glutaraldehyde in anaerobic water for 2-3 days at 4°C. The

641 fixed samples were washed by 0.1 M sodium cacodylate followed by a wash in nanopure water.
642 After washing, the samples were dehydrated with a series of ethanol-water solutions. The
643 ethanol-water solution series included the following dehydration steps: 30% (20 min), 50% (20
644 min), 70% (20 min), 80% (20 min), 90% (20 min) and 100% (3×20min) of 200 proof ethanol.
645 After air-drying, the samples were mounted on double-sided carbon tape and coated with a thin
646 layer 5 nm of Au/Pd or 10 nm of carbon using a Hummer V sputter coater. EDS spectra were
647 treated and analyzed by TEAM EDS 2.0 analysis software (EDAX, NJ, USA) and Microsoft
648 Excel 2016.

649

650 **4.2. Transmission electron microscopy**

651 Transmission electron micrographs were obtained using FEI Tecnai F20 supertwin microscope
652 (TEM, FEI Tecnai G2, FEI, OR, USA) with a 200 kV Schottky field emission gun. The samples
653 were imaged at 80 kV with 1024 × 1024 CCD Gatan camera (Gatan, CA, USA). The samples
654 were fixed by 0.2 M sodium cacodylate, 0.1% CaCl₂·6H₂O and 2.5% glutaraldehyde in aerobic
655 nanopure water for 2-3 days at 4°C. The samples were then washed with washing buffer (0.1 M
656 sodium cacodylate in nanopure water), postfixed with 1% osmium tetroxide in water for 1 hour,
657 washed with aerobic nanopure water, and stained with 1% uranyl acetate for 1 hour. The stained
658 samples were washed with nanopure water and dehydrated with a series ethanol-water solution.
659 The ethanol-water solution series included the following dehydration steps: 30% (20 min), 50%
660 (20 min), 70% (20 min), 80% (20 min), 90% (20 min), and 100% (3×20 min) of 200 proof
661 ethanol. The samples were further dehydrated with propylene oxide:ethanol solvent (50:50, by
662 vol) for 30 min, then with 100% propylene oxide. The epoxy resin used for embedding consisted
663 of diglycerol ether of polypropylene glycol (EmBed 812, DER 736, Electron Microscopy
664 Sciences, EMS #14130, PA, USA), cycloaliphatic epoxide resin (ERL 4221 Electron
665 Microscopy Sciences, EMS #14300, PA, USA), Nonenyl succinic anhydride (NSA, Electron
666 Microscopy Sciences, EMS#14300, PA, USA) and 2-(dimethylamino)ethanol (DMAE, Electron
667 Microscopy Sciences, EMS#14300, PA, USA). The samples were embedded in resin and cut into
668 80 nm thick sections with a diamond knife using Leica Reichert Ultracut E microtome (Reichert
669 Ultracut E microtome, Leica, Germany) with a thickness setting of 50 nm. Thin sections were
670 placed on FCF-200 grids (Electron Microscopy Sciences, Cat# FCF-200-Cu, PA, USA).

671 To determine whether the fixation and embedding protocols introduced any artifacts,
672 photosynthetic biofilms were also harvested without any further processing or staining in the
673 anaerobic chamber. A drop of microbial culture was deposited on LC-200 grid (Electron
674 Microscopy Sciences, Cat#LC-200-Cu, PA, USA) and imaged with JEOL 2010F transmission
675 electron microscope (TEM, JOEL 2010F, JOEL, CA, USA). The JEOL 2010F TEM is equipped
676 with a Schottky field emission gun (FEG) operating at 200 kV and a Gatan energy filter (GIF,
677 Gatan 200, Gatan, CA, USA). The 2010F TEM has micro-diffraction, diffraction pattern in
678 parallel beam, and convergent beam electron diffraction features to allow selected area electron
679 diffraction (SAED) on selected mineral-encrusted bacteria with a high spatial resolution. Gold
680 standard was used as reference for SAED analyses. The high-angle annular dark field detector
681 (HAADF, Gatan, CA, USA) for atomic resolution scanning electron transmission microscopy in
682 the free-lens control mode (STEM) and with an energy dispersive spectrometer (EDS, Bruker
683 silicon drift detector SDD, Bruker, MA, USA) enabled elemental analysis at nanoscale
684 resolution. Images in the TEM and STEM mode were taken by a digital camera (Gatan Orius,

685 Gatan, CA, USA). SAED patterns were imaged using Gatan digiscan unit (Gatan, CA, USA).
686 TEM, STEM and SAED images were recorded and treated using Gatan digital micrograph
687 software (Gatan, CA, USA). EDS spectra were recorded and treated using INCA program
688 (Oxford instruments, UK).

689

690 **4.3. Interpretation of SAED patterns**

691 Different types of manganese minerals in photosynthetic biofilms corresponded to different
692 stages of mineral maturation. HRTEM of the manganese oxide nanocluster surrounding a cell
693 (Fig. 3) showed polycrystalline minerals with a uniform lattice fringe that corresponded to the
694 (116) plane with interplanar spacing of 2.71 Å of calcium manganese oxide (ICDD-00-053-
695 0092). The SAED patterns of minerals that were not associated with cell surfaces showed
696 various minerals. One type of manganese mineral had four obvious polycrystalline diffraction
697 rings that could be observed at 3.65 Å, 3.40 Å, 2.88 Å and 1.83 Å, respectively. These
698 corresponded, respectively, to the (112), (211), (220) and the (323) crystal planes of Mn₃O₄
699 (ICDD-03-065-2776) (Fig. 3). Some globular nanocrystals of manganese oxide outside of any
700 microbial surfaces (Fig. 3) showed lattice fringes with the interplanar spacing of 2.26 Å. This
701 matched the characteristic interplanar spacing of the (200) plane of manganese oxide type MnO
702 mineral (ICDD-04-004-3858).

703

704 **5. Concentrations of dissolved species in culture media**

705 Sulfide concentrations were determined by the modified method of Cline⁶² in samples of
706 triplicate cultures for each time point. Briefly, 200 µL of each liquid sample was diluted in 1 ml
707 of 0.05 M zinc acetate. Standards were prepared from 1 mM anaerobic stock solution of Na₂S
708 diluted by 0.05 M zinc acetate. The concentration of Na₂S stock solution was verified by
709 precipitating an exact volume of Na₂S with an excess volume of 0.3 M silver nitrate. 600 µL of
710 the precipitated sample were transferred and reacted with 10 µL of diamine reagent. After 20
711 minutes reaction time in the dark, the absorbance was measured by a multi-mode reader
712 spectrophotometer (BioTek, Synergy 2, Winooski, VT, USA) at 670 nm.

713 The concentrations of sulfate, nitrite and nitrate in the samples of the liquid medium from
714 triplicate cultures were determined by ion chromatography (IC, Dionex ICS-16000 equipped
715 with an auto-sampler Dionex AS-DV, ThermoFisher, USA), guard column (Dionex Ion
716 PacTMAG22, RFICTM, Guard 2x50 mm, Thermo Fisher, USA), analytical column (Dionex Ion
717 PacTMAS22, RFICTM, Analytical 2X250mm, Thermo Fisher, USA) and a trap column for metals
718 (Dionex Ion PacTMMFC-1, RFICTM, trap column, metal free, 3x27mm, Thermo Fisher, USA).
719 All samples were filtered anaerobically through 0.2 µm pore-size filters (Acrodisc 25 mm syringe
720 filter, PALL corporation, MA, USA) and stored at -20 °C. Chloride ion was solid-phase
721 extracted from all samples using a Ag/H cartridge (Dionex OnGuardTM II Ag/H, 2.5 cc cartridge,
722 Thermo Fisher, USA) before the analysis. The removal of chloride ion affected the lower
723 detection limit for phosphate, but not for sulfate and nitrate. The limits of detection for sulfate,
724 nitrate and nitrite, respectively, were 20 µg/L, 20 µg/L and 10 µg/L respectively.

725 Total dissolved manganese concentrations in the liquid culture media from triplicate
726 cultures were determined by inductively coupled plasma-mass spectrometry (ICP-MS, Agilent
727 7500, Agilent, USA). All samples were filtered through 0.2 µm pore-size filters (Acrodisc 25 mm
728 syringe filter, PALL corporation, MA, USA), and acidified with 2% high purity HCl
729 (hydrochloric acid 30%, Sigma Aldrich, suprapur- end Millipore, 100318, MO, USA) and stored

730 at -20 °C. All samples were diluted with high purity 2% HCl (hydrochloric acid 30%, Sigma
731 Aldrich, suprapur- EMD Millipore, 100318, MO, USA) before the analysis. These measurements
732 did not reveal any oxidized manganese in the liquid phase.

733 Dissolved manganese in the liquid phase was also measured by leucoberbelin blue (LBB)
734 assay⁶³ and iodometric method⁶⁴. Oxidized manganese in the liquid phase includes any soluble
735 valence state of Mn that can be filtered through the 0.2 µm pore filter. We used the iodometric
736 method^{64,65} to determine Mn oxidation state including Mn(II), Mn(III), Mn(IV) and Mn(VII).
737 Again, none of the measurements detected oxidized manganese in the liquid phase. LBB assay
738 was also used to quantify the concentrations of oxidized manganese in biofilms. These
739 concentrations were detected as oxidizing equivalents of KMnO₄ (Section 6).

740 The concentration of peroxide was measured in triplicate samples of microbial biofilms
741 and sterile controls incubated in the light with 1 mM Mn(II) and 50 µM Na₂S using a peroxidase
742 activity assay kit (Sigma Aldrich, MAK092, MO, USA). The standard curve was measured using
743 different dilutions of the H₂O₂ standard (Sigma Aldrich, MAK092C, MO, USA) in sterile culture
744 medium mixed with the reaction mix composed of 2 µL fluorescent peroxidase substrate (Sigma
745 Aldrich, MAK092B, MO, USA) and 48 µL of HRP positive control (Sigma Aldrich, MAK092D,
746 MO, USA). A 100 µL of each diluted H₂O₂ standard and the samples were distributed into
747 microplate wells. The plate was incubated at 37°C and the initial measurement (T_{initial}) was
748 measured after 3 minutes by multi-mode reader spectrophotometer (BioTek, synergy 2,
749 Winooski, VT, USA) at 570 nm. The absorbance was measured every 3 minutes until the value
750 of the most active sample exceeded the end linear range of the standard curve. We did not detect
751 any H₂O₂ in the incubations or sterile controls. The limit of detection of H₂O₂ using colorimetric
752 detection was 0.1 nM.

753

754 **6. Quantification of biofilms and oxidized manganese in biofilms**

755 The amount of biofilm was measured by crystal violet (CV) staining using the modified assay of
756 O'Toole⁶⁶. Briefly, biofilms from triplicate serum bottles were harvested at each time point and
757 centrifuged aerobically at 10,000 rpm for 30 minutes. The supernatant was decanted and 0.5 ml
758 of 0.1% of aqueous crystal violet added (crystal violet, Sigma Aldrich, ACS reagent, ≥ 90 %
759 anhydrous basis, C6158, MO, USA). The stained biofilm was incubated in the dark at room
760 temperature for 24 hours, washed 15 times with nanopure water, and air-dried. After drying, 0.5
761 ml of 30% acetic acid (37 % Acetic acid, Sigma Aldrich, ACS reagent, ≥ 99.7%, 695092, MO,
762 USA) was added to the samples and left to react at room temperature for 30 minutes. Acetic acid
763 solubilized all crystal violet molecules bound to peptidoglycan and exopolysaccharide. Thus, the
764 solubilized CV corresponds to the biomass in biofilms. The collected solubilized CV was filtered
765 through 0.2 µm pore-size filters (Acrodisc 25 mm syringe filter, PALL corporation, MA, USA)
766 and 200 µl of the solution was transferred into a microtiter plate. The absorbance of the samples
767 was measured at 550 nm using a spectrophotometer (BioTek, synergy 2, Winooski, VT, USA).

768 Oxidized manganese in biofilms was quantified by the leucoberbelin blue assay (LBB).
769 Biofilms were inoculated from frozen stocks into triplicate serum bottles that contained 25 ml or
770 50 ml of MFGL medium and incubated for one-, two or three weeks. Biofilms from the frozen
771 stock (~ 5 mg) were washed 10 times with anaerobic nanopure water to remove any glycerol,
772 inoculated into the culture medium and the medium was immediately flushed with 20 % CO₂/80
773 % N₂ (v/v) for 1 hour. The biofilms grew for two weeks in the light, at which point, biofilms (~ 5

774 mg) were transferred into serum bottles that each contained 25 ml of the fresh MFGL medium.
775 Three bottles were incubated in the light, three in the dark and all biofilms were harvested after
776 one or two weeks by pipetting and centrifugation in the anaerobic glove box. After the LBB
777 assay, all analyzed samples were air-dried for > 24 h and weighed. The one-week old biofilms
778 weighed 16-18 mg, the two-week old biofilms weighed 19-21 mg. A separate experiment
779 quantified the amount of oxidized manganese in duplicate 25 ml cultures of three-week old
780 biofilms that had been inoculated with ~ 0.1 mg of the washed material from frozen culture
781 stocks and weighed <0.3 mg at the end of the experiment. In contrast to the experiments that
782 yielded samples for XRD, XPS, SEM and TEM analyses, these experiments involved at most
783 one successive transfer of biofilms after the inoculation from frozen stocks of biofilms enriched
784 as described in Section 1.1.

785 The working reagent was prepared as 0.04% LBB in 45 mM acetic acid and stored at 4°C
786 overnight in a light-proof container. Potassium permanganate (KMnO₄) 1 mM stock solution was
787 freshly prepared in water and standards (5, 10, 15, 20, 40, 50 μM) were prepared by diluting the
788 stock solution in water. The samples were incubated for 20 minutes in 0.75 ml of the 0.04% LBB
789 working reagent in the dark at room temperature and centrifuged for 90 s at 10,000 rcf to remove
790 the biofilm and mineral particulates from the solution. The absorbance of the supernatant was
791 measured on a spectrophotometer at 618 nm. To determine whether some manganese was
792 oxidized in the dark, ~ 5 mg of the biofilm stock was inoculated into sterile MFGL in the dark
793 for two weeks which detected on average 0.02 μM oxidizing equivalent per 5 mg of biofilm.
794 Control experiments assayed the concentration of oxidized manganese in FGL enrichment
795 cultures that contained 1 mM sulfide and 1 mM MnCl₂ and did not detect any.

796

797 **7. Oxygen concentration**

798 To determine how much oxygen can diffuse into the cultures through the butyl rubber caps, we
799 used our in-house developed oxygen sensor⁶⁷, based on the fluorescence lifetime of 5,10,15,20-
800 tetrakis(pentafluorophenyl)-21H,23H-porphine palladium(II)⁶⁸. The sensor can detect changes in
801 the partial pressure of oxygen that are smaller than 1 μbar and its main sensitivity region is 0-100
802 μatm⁶⁷.

803 Experiments were conducted to quantify the oxygen concentration in the cultures and the
804 maximum amount of oxygen inflow. First, the partial pressures of oxygen in the headspaces of
805 photosynthetic cultures, sterile controls incubated in the light, and dark control cultures were
806 measured automatically for 14 days. All serum bottles contained 100 mL of the medium reduced
807 by 50 μM Na₂S (Extended Data Figure 1). The partial pressure of oxygen in the headspaces of
808 the bottles did not increase or fluctuate by more than 2 μbar over the course of the growth
809 experiment. The main sources of noise were daily thermal fluctuations (high frequency
810 component) and sensor aging (low frequency component). The upper limit for the partial
811 pressure of oxygen in the headspace is 2 μbar, measured in the beginning of the experiment. This
812 partial pressure was lower than 0.5 μbar during most of the experiment. This corresponds to a
813 maximum dissolved molecular oxygen concentration of 2.6 nM, assuming the equilibrium
814 between O₂ in the headspace and O₂ dissolved in the culture medium according to Henry's law.

815 In an additional test, we incubated biofilms in the light in the anaerobic chamber under a
816 5%CO₂: 5%H₂: balN₂ (v/v/v) atmosphere. The partial pressure of oxygen in the chamber was
817 below 1 ppm, as opposed to 21% above the butyl rubber stoppers of the cultures that were

818 incubated outside of the chamber. Therefore, orders of magnitude less oxygen is expected to
819 diffuse into the cultures. The biofilms were grown with and without the addition of 1 mM Mn(II)
820 and the culture medium was reduced with 20 μ M Na₂S. After two weeks of incubation, the
821 biofilms were harvested and analyzed by XRD. Manganese oxides and carbonates phases formed
822 in biofilms incubated with Mn(II), elemental sulfur formed in biofilms grown without Mn(II).
823 The formation of detectable quantities of manganese oxides in photosynthetic cultures incubated
824 in the anaerobic glove box further demonstrated the negligible role of oxygen diffusion in the
825 oxidation of manganese.

826

827 **8. Acquisition of phototrophy in green sulfur bacteria**

828 Phototrophy within stem group green sulfur bacteria (GSB) and stem group green non-sulfur
829 bacteria (GNS) could have been acquired at any point before their post-GOE diversification
830 events. Without additional information, it is not possible to infer where along these branches
831 phototrophy was acquired, but the evolutionary history of bacteriochlorophyll biosynthesis may
832 provide a strong clue. Phylogenies of protein families involved in bacteriochlorophyll
833 biosynthesis have a complex evolutionary history across phototrophic lineages, including gene
834 duplications within stem GSB, and multiple HGT events between GSB and GNS lineages⁶⁹.
835 Specifically, the genes encoding BchH and BchM were transferred from within crown GNS to
836 stem GSB, with the gene encoding BchH undergoing a duplication shortly before crown GSB.
837 BchI is also observed to duplicate in the GSB stem, with one paralog being transferred to stem
838 GNS. These observations indicate that phototrophy must have existed in these lineages at the
839 time of any bacteriochlorophyll synthesis gene duplications, or any divergence of an HGT donor
840 lineage. A substantial history of phototrophy within the GSB stem lineage can be inferred from
841 these events (Extended Data Fig. 13). Future molecular clock studies including these gene tree
842 histories may be able to constrain the time interval for phototrophy in the GSB stem; but the Bch
843 protein histories alone suggest that phototrophy within GSB existed much before the appearance
844 of the GSB or GNS crown groups.

845

846

847

848

848 **References**

849

- 850 30 Bekker, A. *et al.* Dating the rise of atmospheric oxygen. *Nature* **427**, 117–120 (2004).
851 31 Balch, W. E. & Wolfe, R. S. New approach to the cultivation of methanogenic bacteria:
852 2-mercaptoethanesulfonic acid (HS-CoM)-dependent growth of *Methanobacterium*
853 *ruminantium* in a pressurized atmosphere. *Appl. Environ. Microbiol.* **32**, 781-791 (1976).
854 32 Sim, M. S., Bosak, T. & Ono, S. Large sulfur isotope fractionation does not require
855 disproportionation. *Science* **333**, 74-77 (2011).
856 33 Sim, M. S., Ono, S., Donovan, K., Templer, S. P. & Bosak, T. Effect of electron donors
857 on the fractionation of sulfur isotopes by a marine *Desulfovibrio sp.* *Geochim.*
858 *Cosmochim. Acta.* **75**, 4244-4259 (2011).
859 34 Liang, J., Bai, Y., Men, Y. & Qu, J. Microbe–microbe interactions trigger Mn (II)-
860 oxidizing gene expression. *The ISME journal* **11**, 67-77 (2017).
861 35 Ljungdahl, L. & Wiegel, J. Working with anaerobic bacteria. *Manual of Industrial*
862 *Microbiology* p. 115-127 American Society for Microbiology. (1986).

45

46

863 36 Pfennig, N. *Rhodocyclus purpureus* gen. nov. and sp. nov., a ring-shaped, vitamin B12-
864 requiring member of the family Rhodospirillaceae. *Int. J. Syst. Evol. Microbiol.* **28**, 283-
865 288 (1978).

866 37 Benson, D. A. *et al.* GenBank. *Nucleic. Acids. Res.* **41**, D36-D42 (2013).

867 38 Caporaso, J. G. *et al.* Global patterns of 16S rRNA diversity at a depth of millions of
868 sequences per sample. . *Proc. Natl. Acad. Sci.* **108**, 4516-4522 (2011).

869 39 Caporaso, J. G. *et al.* QIIME allows analysis of high-throughput community sequencing
870 data. *Nat. Methods* **7**, 335-336 (2010).

871 40 Aronesty, E. Comparison of sequencing utility programs. *Open Bioinformatics J.* **7**, 1-8
872 (2013).

873 41 Edgar, R. C., Haas, B. J., Clemente, J. C., Quince, C. & Knight, R. UCHIME improves
874 sensitivity and speed of chimera detection. *Bioinformatics* **27**, 2194-2200 (2011).

875 42 McDonald, D. *et al.* An improved Greengenes taxonomy with explicit ranks for
876 ecological and evolutionary analyses of bacteria and archaea. *ISME J* **6**, 610-618 (2012).

877 43 Price, M. N., Dehal, P. S. & Arkin, A. P. FastTree 2-approximately maximum-likelihood
878 trees for large alignments. *PLoS One* **5**, e9490 (2010).

879 44 Segata, N., Izard, J., Waldron, L., Gevers, D., Miropolsky, L., Garrett, W. S., &
880 Huttenhower, C. Metagenomic biomarker discovery and explanation. *Genome*
881 *biology*, *12*(6), R60. (2011).

882 45 Momper, L. M., Reese, B. K., Carvalho, G., Lee, P. & Webb, E. A. A novel cohabitation
883 between two diazotrophic cyanobacteria in the oligotrophic ocean. *ISME J* **9**, 882-893
884 (2015).

885 46 Bolger, A. M., Lohse, M. & Usadel, B. Trimmomatic: a flexible trimmer for Illumina
886 sequence data. *Bioinformatics* **30**, 2114-2120 (2014).

887 47 Li, H. *et al.* The Sequence Alignment/Map format and SAMtools. *Bioinformatics* **25**,
888 2078-2079 (2009).

889 48 Laczny, C. C. *et al.* VizBin - an application for reference-independent visualization and
890 human-augmented binning of metagenomic data. *Microbiome* **3**, 1 (2015).

891 49 Parks, D. H., Imelfort, M., Skennerton, C. T., Hugenholtz, P. & Tyson, G. W. CheckM:
892 assessing the quality of microbial genomes recovered from isolates, single cells, and
893 metagenomes. *Genome. Res.* **25**, 1043-1055 (2015).

894 50 Huntemann, M. *et al.* The standard operating procedure of the DOE-JGI Microbial
895 Genome Annotation Pipeline (MGAP v.4). *Stand. Genomic. Sci.* **10**, 1-6 (2015).

896 51 Mansor, M., & Macalady, J. L. Draft genome sequence of lampenflora *Chlorobium*
897 *limicola* strain Frassasi in a sulfidic cave system. *Genome announcements*, *4*(3), e00357-
898 16. (2016).

899 52 Ridge, J. *et al.* A multicopper oxidase is essential for manganese oxidation and laccase-
900 like activity in *Pedomicrobium* sp. ACM 3067. *Environ. Microbiol.* **9**, 944-953 (2007).

901 53 Anderson, C. R. *et al.* Mn (II) oxidation is catalyzed by heme peroxidases in
902 *Aurantimonas manganoxydans* strain SI85-9A1 and *Erythrobacter* sp. strain SD-21.
903 *Appl. Environ. Microbiol.* **75**, 4130-4138 (2009).

904 54 Altschul, S. F. *et al.* Gapped BLAST and PSI-BLAST: a new generation of protein
905 database search programs. *Nucleic. Acids. Res.* **25**, 3389-3402 (1997).

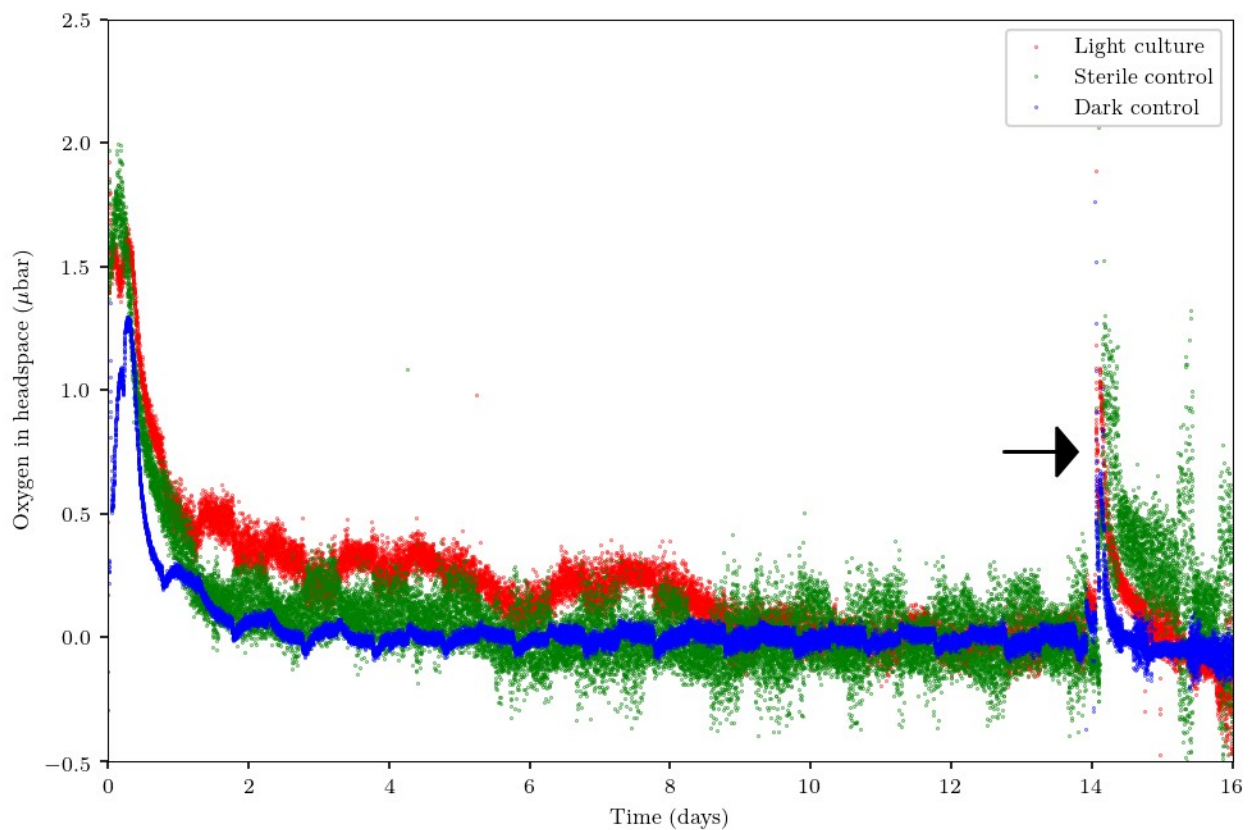
- 906 55 Nesbitt, H. & Banerjee, D. Interpretation of XPS Mn (2p) spectra of Mn oxyhydroxides
907 and constraints on the mechanism of MnO₂ precipitation. *Am. Mineral.* **83**, 305-315
908 (1998).
- 909 56 Oku, M., Hirokawa, K. & Ikeda, S. X-ray photoelectron spectroscopy of manganese—
910 oxygen systems. *J. Electron. Spectrosc. Relat. Phenom.* **7**, 465-473 (1975).
- 911 57 Han, X., Zhang, J., Du, F., Cheng, J., Chen, J. Porous calcium–manganese oxide
912 microspheres for electrocatalytic oxygen reduction with high activity. *Chem. Sci.* **4**, 368-
913 376 (2013).
- 914 58 Audi, A. A. & Sherwood, P. M. A. Valence-band x-ray photoelectron spectroscopic
915 studies of manganese and its oxides interpreted by cluster and band structure calculations.
916 *Surf. Interface. Anal.* **33**, 274-282 (2002).
- 917 59 Toupin, M., Brousse, T. & Bélanger, D. Charge storage mechanism of MnO₂ electrode
918 used in aqueous electrochemical capacitor. *Chem. Mater.* **16**, 3184-3190 (2004).
- 919 60 Foord, J., Jackman, R. & Allen, G. An X-ray photoelectron spectroscopic investigation
920 of the oxidation of manganese. *Philos. Mag. A.* **49**, 657-663 (1984).
- 921 61 Božin, E. S. *et al.* Structure of CaMnO₃ in the range 10K ≤ T ≤ 550 K from neutron time-
922 of-flight total scattering. *J Phys Chem Solids* **69**, 2146-2150 (2008).
- 923 62 Cline, J. D. Spectrophotometric determination of hydrogen sulfide in natural waters.
924 *Limnol. Oceanogr.* **14**, 454-458 (1969).
- 925 63 Krumbein WE, Altman HJ. A new method for the detection and enumeration of
926 manganese-oxidizing and -reducing microorganisms. *Helgol Wiss Meeresunters* **25**:347–
927 356 (1973).
- 928 64 Murray JW, Balistrieri LS, Paul B. The oxidation state of manganese in marine sediments
929 and ferromanganese nodules. *Geochim. Cosmochim. Acta* **48**: 1237-1247 (1984).
- 930 65 Pierre Anschutz, Karine Dedieu, Franck Desmazes, Gwénaëlle Chaillou. Speciation,
931 oxidation state, and reactivity of particulate manganese in marine sediments. *Chem. Geol.*
932 **218**: 265-279 (2005).
- 933 66 Pajusalu, M., Borlina, C. S., Seager, S., Ono, S. & Bosak, T. Open-source sensor for
934 measuring oxygen partial pressures below 100 microbars. *PLoS ONE* **13**, e0206678
935 (2018).
- 936 68 Lehner, P. *et al.* LUMOS--A sensitive and reliable optode system for measuring
937 dissolved oxygen in the Nanomolar Range. *PLoS One* **10**, e0128125 (2015).
- 938 69 Sousa, F. L., Shavit-Grievink, L., Allen, J. F. & Martin, W. F. Chlorophyll biosynthesis
939 gene evolution indicates photosystem gene duplication, not photosystem merger, at the
940 origin of oxygenic photosynthesis. *Genome Biol. Evol.* **5**, 200–216 (2012).
- 941 70 Gibson, J. A. E. *et al.* Geochemistry of ice-covered, meromictic Lake A in the Canadian
942 High Arctic. *Aquat. Geochem.* **8**, 97–119 (2002).
- 943 71 Green, W. J., Ferdelman, T. G. & Canfield, D. E. Metal dynamics in Lake Vanda (Wright
944 Valley, Antarctica) *Chem. Geol.* **76**, 85-94 (1989).
- 945 72 Dickman, M. & Ouellet, M. Limnology of Garrow Lake, NWT, Canada. *Polar Rec* **23**,
946 531-549 (1987).
- 947 74 Gallagher, J. B. *Antarctic Nutrient Cycles and Food Webs* (eds. W. R. Siegfried, P. R.
948 Condy, & R. M. Laws) (Springer, 1985).

949 75 Savvichev, A. S. *et al.* Microbial processes of the carbon and sulfur cycles in an ice-
 950 covered, iron-rich meromictic lake Svetloe (Arkhangelsk region, Russia). *Environ.*
 951 *Microbiol.* **19**, 659-672 (2007).
 952 76 Tebo, B. M. Manganese (II) oxidation in the suboxic zone of the Black Sea. *Deep-Sea*
 953 *Res.* **38**, S883-S905 (1991).
 954 77 Su, J. *et al.* CotA, a multicopper oxidase from *Bacillus pumilus* WH4, exhibits
 955 manganese-oxidase activity. *PLoS One* **8**, e60573 (2013).
 956 78 Su, J. *et al.* Catalytic oxidation of manganese (II) by multicopper oxidase CueO and
 957 characterization of the biogenic Mn oxide. *Water Res.* **56**, 304-313 (2014).

958

959

960



961

962

963

964

965

966

967

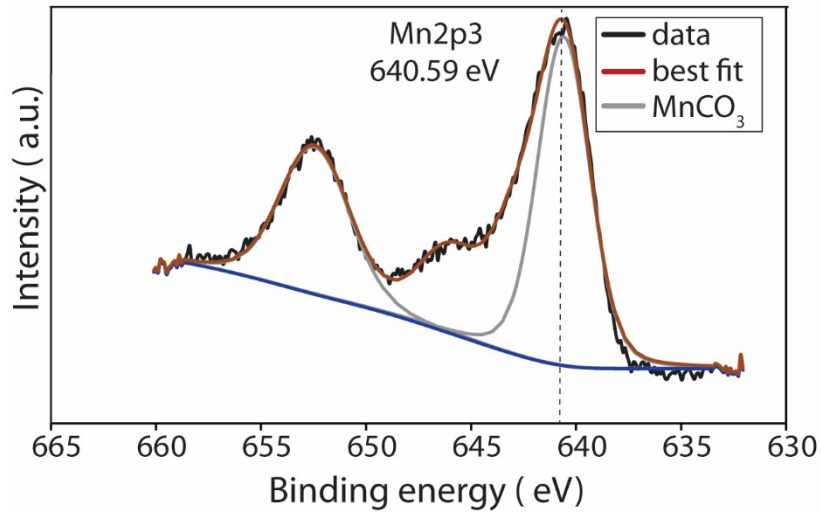
968

969

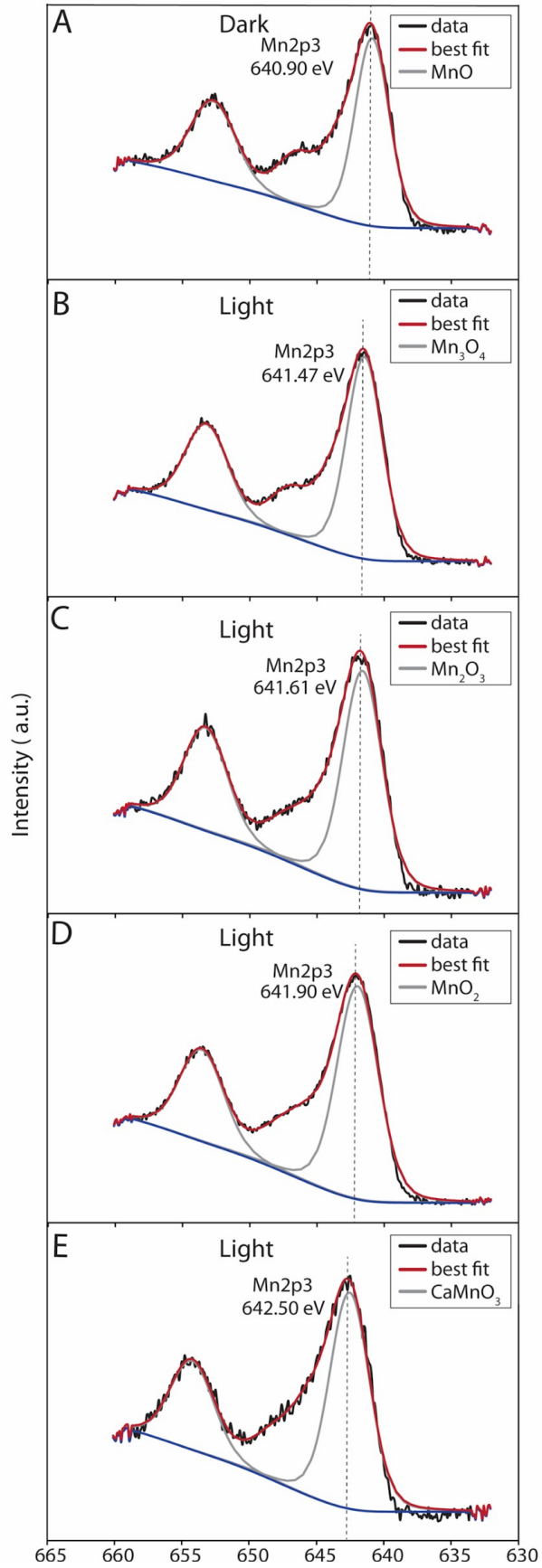
970

Extended Data Figure 1. Partial pressure of oxygen in the headspace of enrichment cultures and dark controls. Oxygen concentration (μatm) measured in the headspaces of 150 ml serum bottles that contained 100 ml of MFGL medium, 50 μM sulfide and 1 mM MnCl_2 . One inoculated culture was incubated in the light (red points), another one) in the dark (blue points). The sterile control (green points) was incubated in the light. Individual points are measurements by the oxygen sensor taken each 48.2 s. To control for sensor drift and recalibrate sensor zero point, the bottles were flushed with oxygen-free N_2 on day 14 (black arrow) after the inoculation. The fluorescence reading value after the stabilization was set as zero. The diurnal oscillations in O_2 concentration reflect temperature changes induced by the

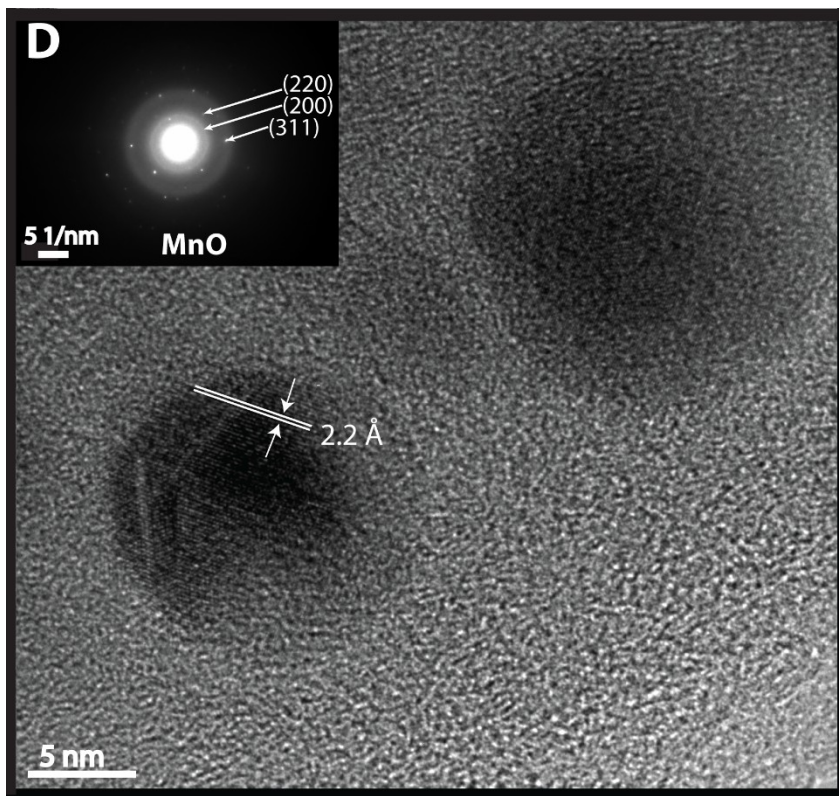
971 proximity to the light bulb with a 12:12 h day/night cycle. Oxygen concentrations in all
972 cultures were lower than 1 nmol at all times after ~ 12 h and before the flushing on day 14.
973
974
975
976



977
978 **Extended Data Figure 2.** X-ray photoelectron spectroscopy (XPS) analysis for the 2p spectral
979 region of Mn in sterile control incubated in the light for two weeks. The Mn₂p_{3/2} main peak of
980 the sample fits the MnCO₃ standard at binding energy of 640.59 eV that corresponds to the redox
981 state of Mn(II).
982
983

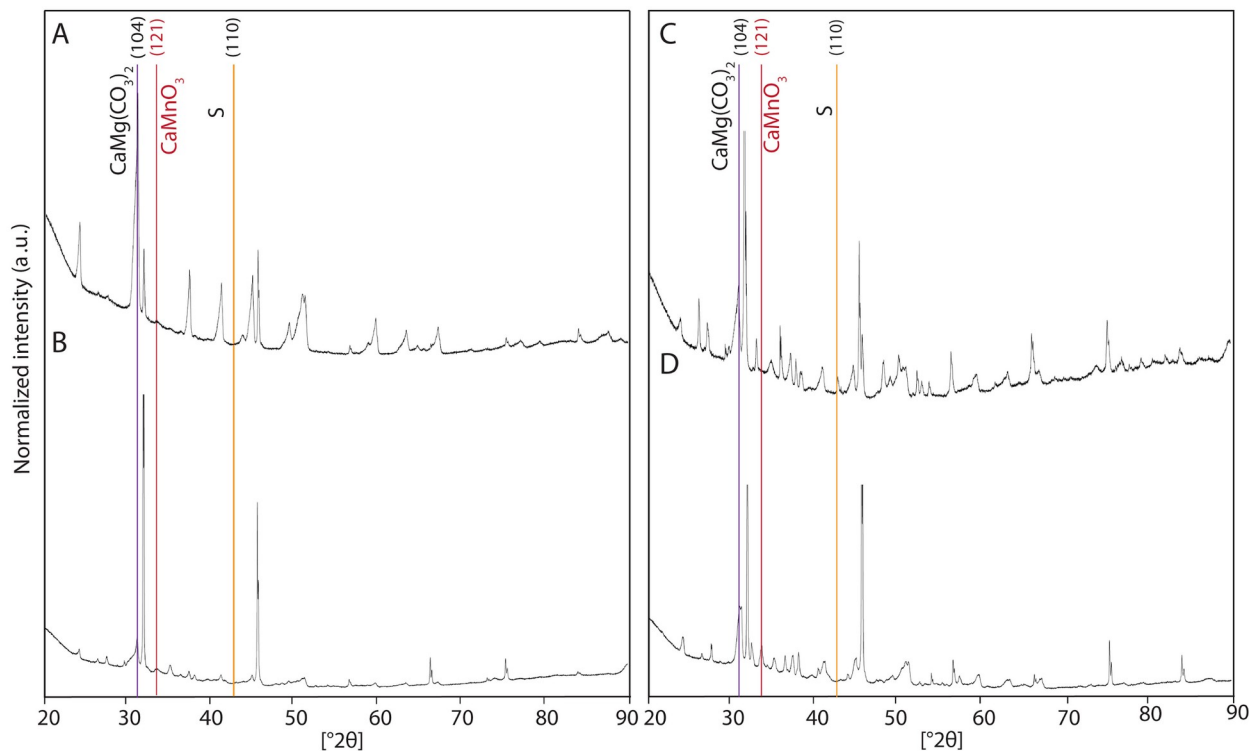


985 **Extended Data Figure 3.** X-ray photoelectron spectra (XPS) of the 2p spectral region of Mn in
 986 two-week old microbial cultures. A: Biofilm incubated in the dark. The Mn2p_{3/2} main peak of the
 987 sample fits the MnO standard at binding energy of 640.90 eV that corresponds to the redox state
 988 of Mn(II). B: Biofilm incubated in the light. The Mn2p_{3/2} main peak of the sample fits the Mn₃O₄
 989 standard at binding energy of 641.47 eV that corresponds to Mn(III) and Mn(II). C: Biofilm
 990 incubated in the light (a different region). The Mn2p_{3/2} main peak of the sample fits the Mn₂O₃
 991 standard at binding energy of 641.61 eV that corresponds to Mn(III). D: Biofilm incubated in the
 992 light (a different region). The Mn2p_{3/2} main peak of the sample fits MnO₂ standard at binding
 993 energy of 641.90 eV that corresponds to redox state of Mn(IV). E: Biofilm incubated in the light.
 994 The Mn2p_{3/2} main peak of the sample fits the CaMnO₃ standard at binding energy of 642.50 eV
 995 that corresponds to Mn(IV).
 996
 997

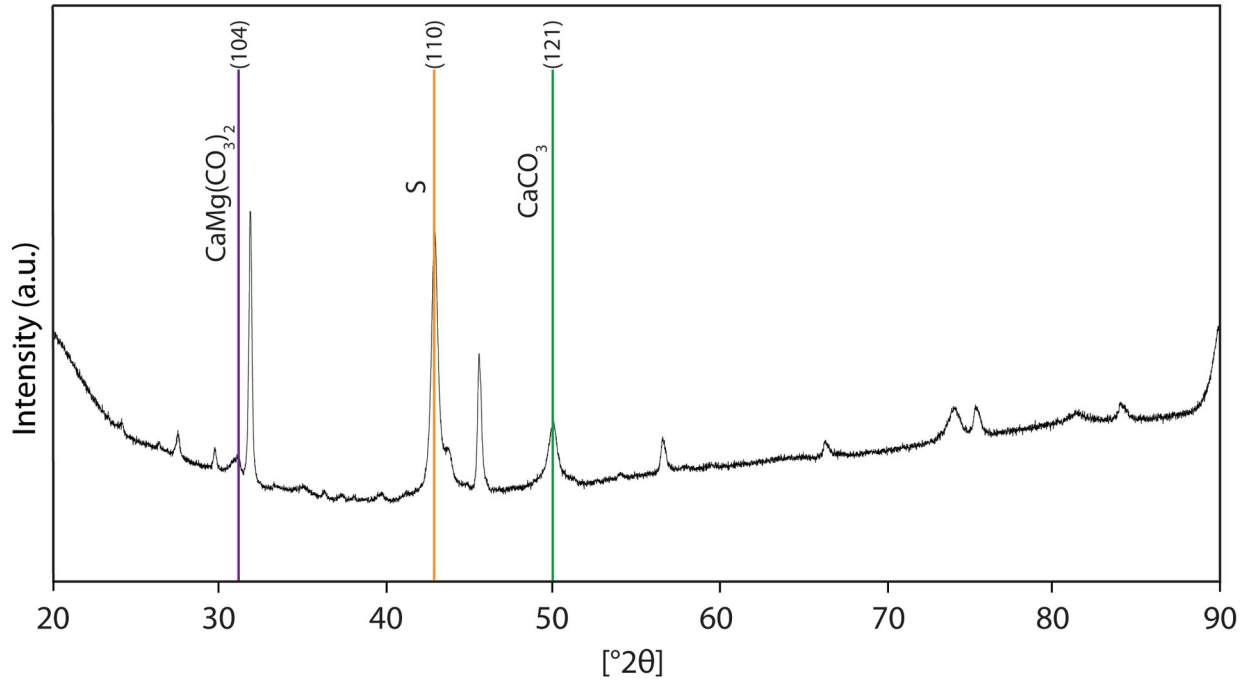


998
 999 **Extended Data Fig. 4.** HRTEM and SAED of minerals found within biofilms, but not on cell
 1000 surfaces. The indexes of the SAED pattern correspond to MnO with d-spacing of 2.2 Å.
 1001
 1002

1003
1004

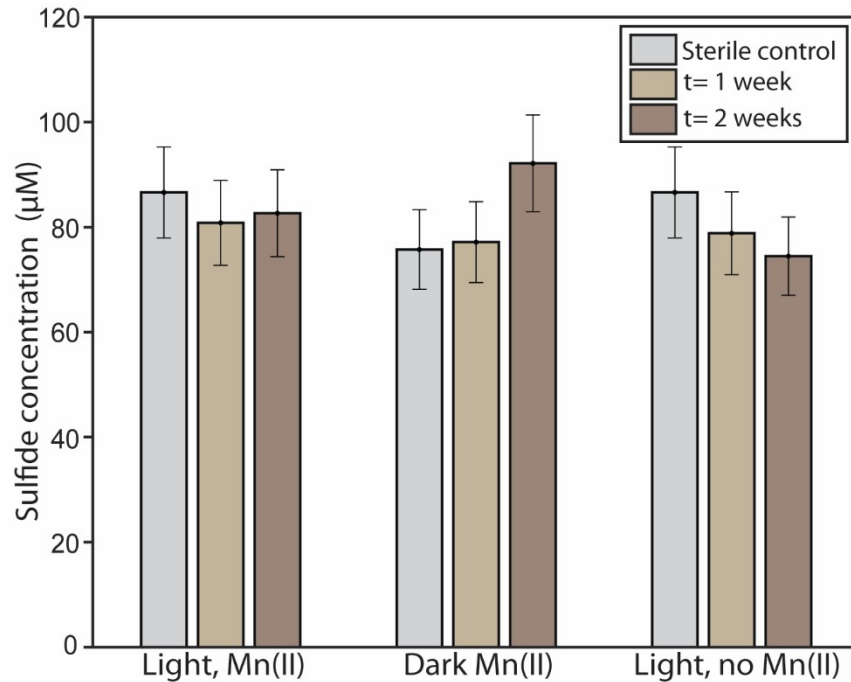


1005
1006 **Extended Data Figure 5.** X-ray diffraction spectra of biofilm samples incubated in the light for
1007 two weeks. These biofilms were not treated to remove manganese oxides before inoculation. A: 1
1008 mM Mn(II) and 0.05 mM Na₂S. B: 0.1 mM Mn(II) and 0.05 mM Na₂S. C: 1 mM Mn(II) and 1
1009 mM Na₂S. D: 1 mM Mn(II) and 0.25 mM Na₂S. Purple line shows the highest intensity peak at
1010 2θ of 30.870° for the basal reflection of (104) plane of dolomite, CaMg(CO₃)₂. Red line shows
1011 the highest intensity peak at 2θ of 33.867° for the basal reflection of (121) plane of CaMnO₃.
1012 Orange line shows the highest intensity peak at 2θ of 42.845° for the basal reflection of (110)
1013 plane of elemental sulfur, S°.



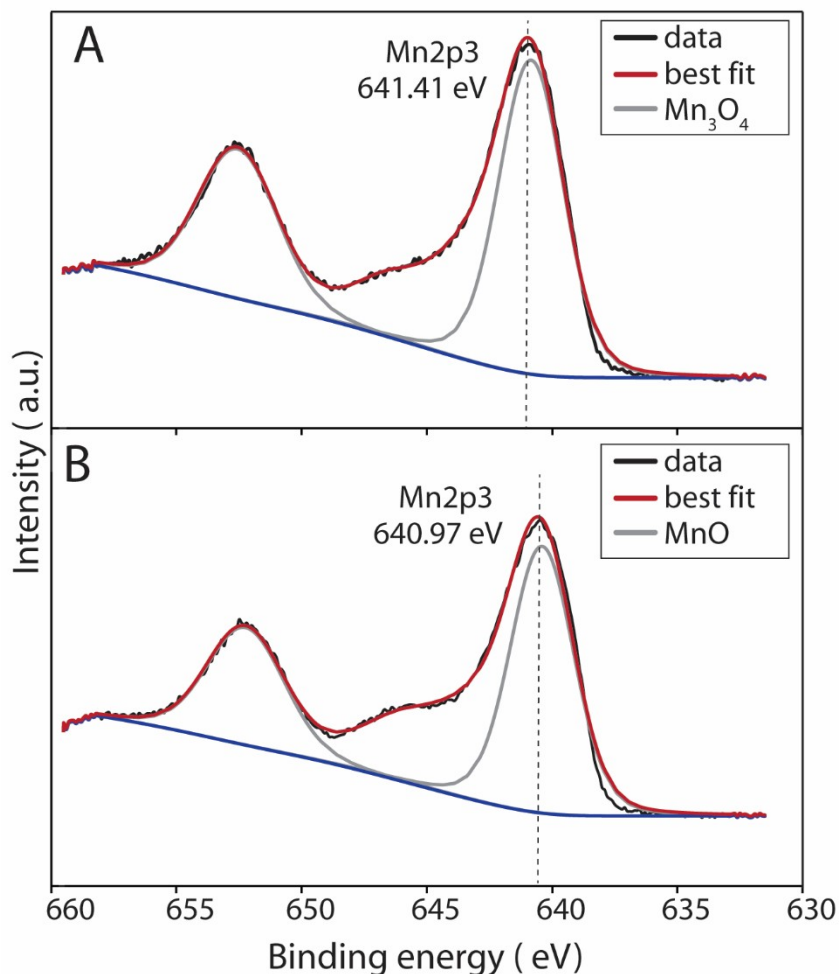
1014
 1015 **Extended Data Figure 6.** XRD of a biofilm incubated with 0.05 mM Na₂S and no Mn(II) in the
 1016 light for 2 weeks. The inoculum for this experiment was not treated to remove manganese
 1017 oxides. Purple line shows the highest intensity peak at 2 Θ of 30.870° for the (104) basal
 1018 reflection of CaMg(CO₃)₂. Orange line shows the highest intensity peak at 2 Θ of 42.845° for the
 1019 (110) basal reflection of S°. Green line shows the highest intensity peak at 2 Θ of 51.051° for the
 1020 (121) basal reflection of CaCO₃.

1021
 1022
 1023
 1024
 1025



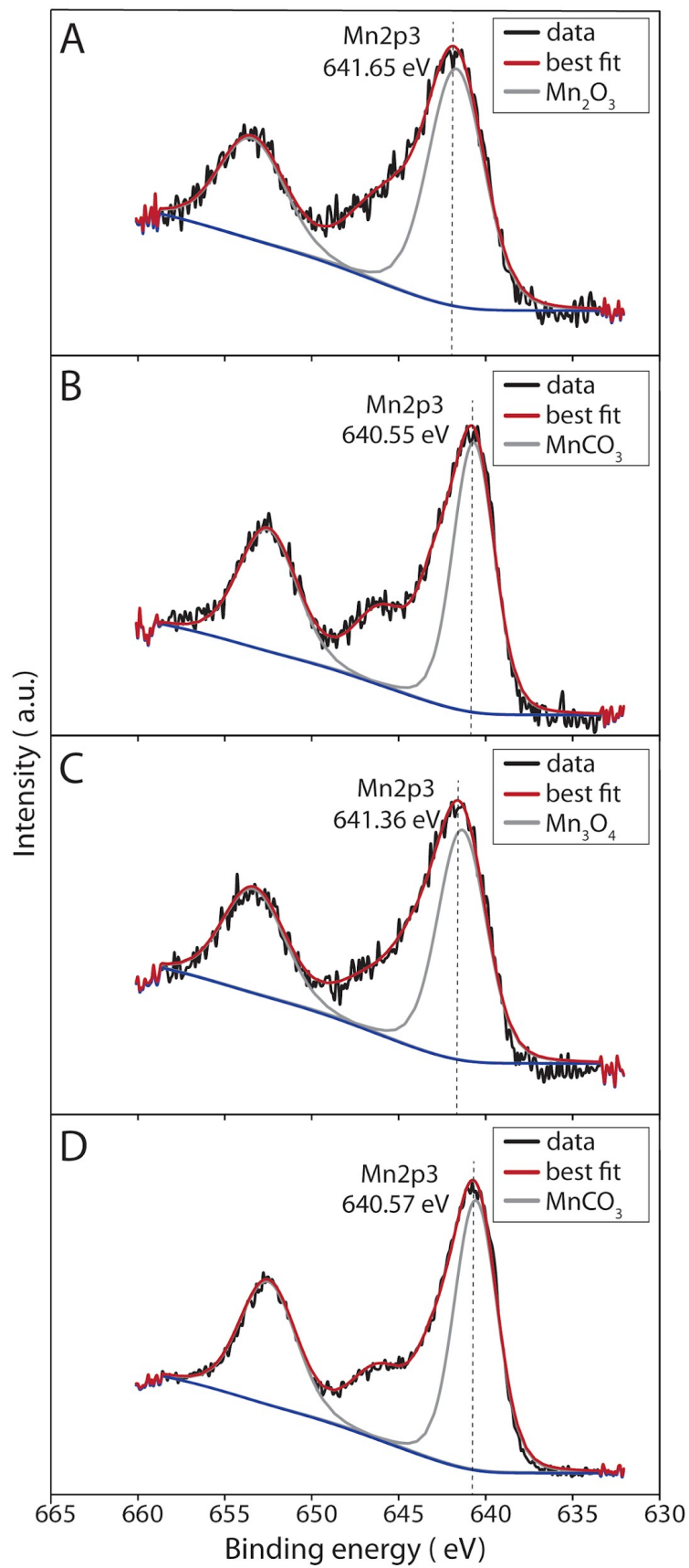
1026
1027
1028
1029
1030
1031
1032
1033
1034
1035
1036

Extended Data Figure 7. Sulfide concentration in biofilms and sterile controls over the course of a two-week experiment. “Light, Mn” refers to biofilms grown with 1 mM Mn(II) and 0.05 mM initial Na₂S. “Dark, Mn” refers to biofilms grown with 1 mM Mn(II) and 0.05 mM initial Na₂S in the dark. “Light, no Mn” refers to biofilms grown in the light at a 12:12h day/night cycle without added MnCl₂ and with 0.05 initial mM Na₂S. The uninoculated media (sterile controls) were incubated under chemical and physical conditions that matched the corresponding cultures (dark, light, no added manganese beyond that in the trace metal solution). The concentrations of sulfide in sterile controls were measured after two weeks. Error bars show standard deviations in triplicate bottles.



1037
 1038 **Extended Data Figure 8.** Test of Mn-oxidizing activity in cell suspensions of photosynthetic
 1039 cultures enriched under two different conditions. Shown are results of XPS analysis of the 2p
 1040 spectral region of Mn. A. Culture enriched on 1 mM Mn(II) and 0.05 mM H₂S (Condition 1).
 1041 The Mn2p_{3/2} main peak of the sample fits Mn₃O₄ standard at binding energy of 641.41 eV. This
 1042 corresponds to Mn(II) and Mn(III). B: Culture enriched on 1 mM H₂S (Condition 2). The
 1043 Mn2p_{3/2} main peak of the sample fits MnO standard at binding energy of 640.97 eV and
 1044 corresponds to the redox state Mn(II). Detailed experimental protocol is described in section 2.2.
 1045 and summarized in Extended Data Table 3.

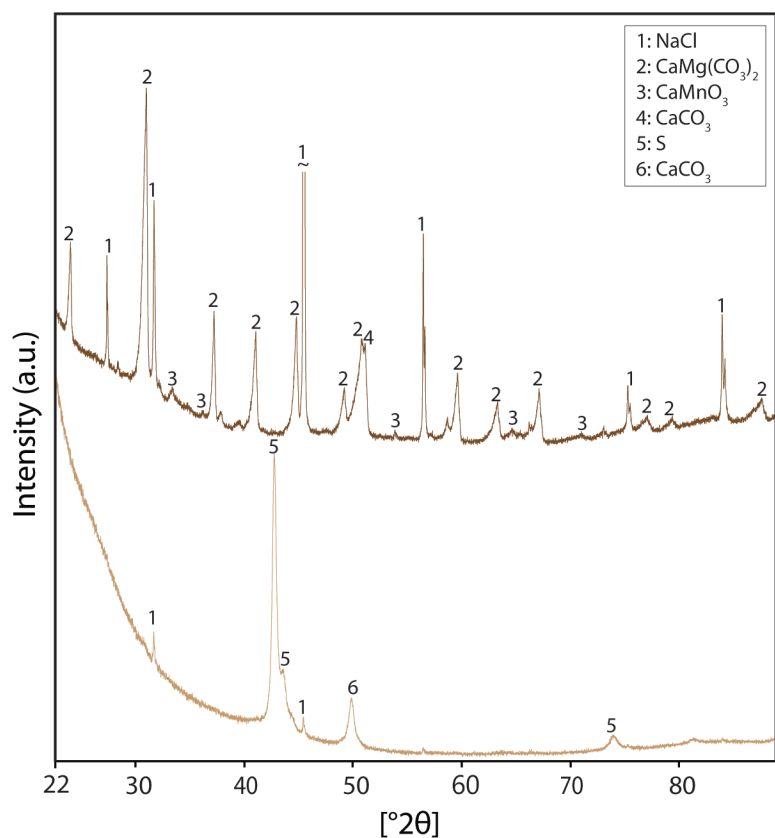
1046
 1047



1048

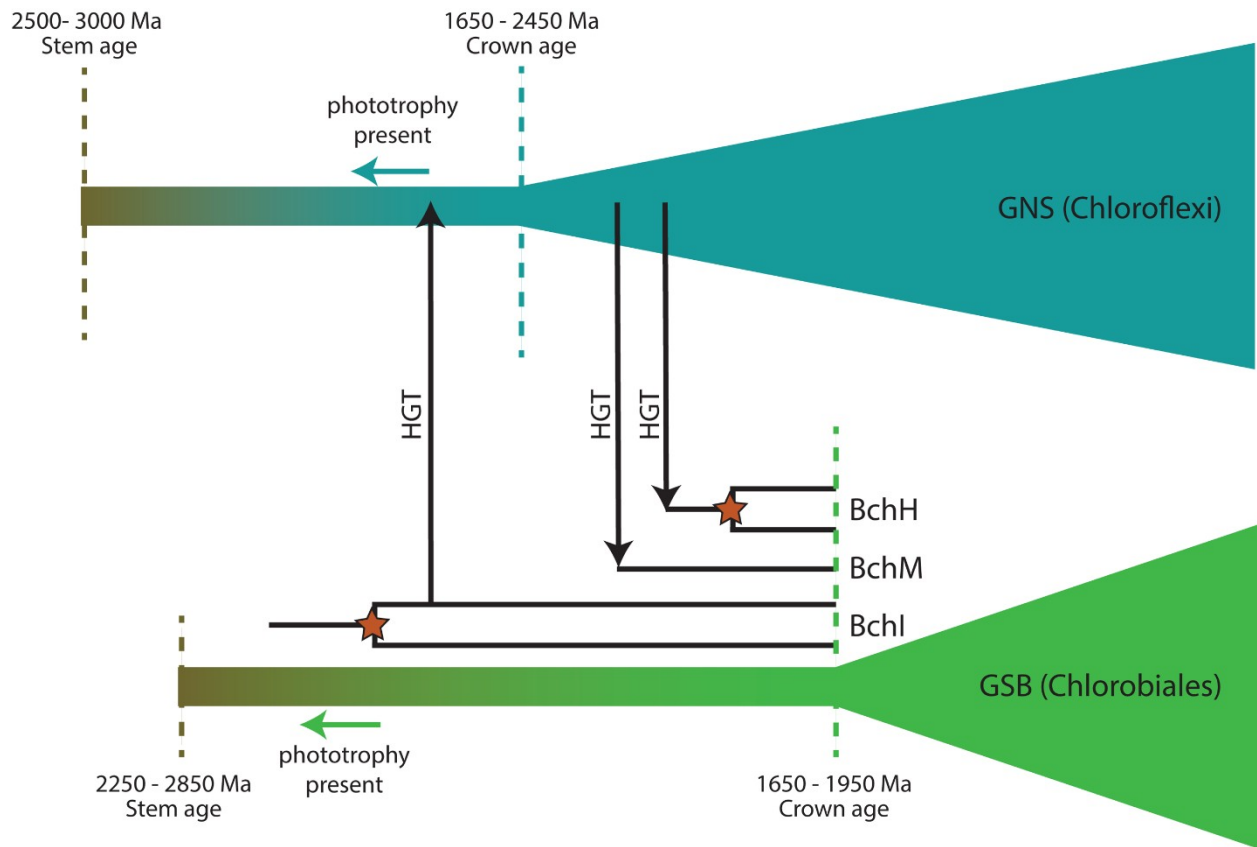
67
68

1049 **Extended Data Figure 9.** Test of Mn-oxidizing activity in cell suspensions of pure cultures and
 1050 co-cultures of *Chlorobium limicola* (*Cl*), *Chlorobaculum tepidum* (*Ct*), and *Geobacter lovleyi*
 1051 (*Gl*). Shown are results of XPS analysis of the 2p spectral region of Mn. A. *Cl*, *Ct* and *Gl*. The
 1052 Mn2p_{3/2} main peak of the sample fits Mn₂O₃ standard at binding energy of 641.65 eV. This
 1053 corresponds to a valence state of Mn(III). B: *Cl* and *Ct*. The Mn2p_{3/2} main peak of the sample fits
 1054 MnCO₃ standard at binding energy of 640.55 eV and corresponds to the redox state Mn(II). C: *Cl*
 1055 and *Gl*. The Mn2p_{3/2} main peak of the sample fits Mn₃O₄ standard at binding energy of 641.36eV.
 1056 D: *Ct* and *Gl*. The Mn2p_{3/2} main peak of the sample fits MnCO₃ standard at binding energy of
 1057 640.57 eV Detailed experimental protocol is described in section 2.2.1. All co-cultures were
 1058 grown with 1 mM Mn(II) and 0.05 mM H₂S for 2 weeks in the light.



1059 **Extended Data Figure 10.** X-ray diffraction spectra of biofilms. Top spectrum: biofilms
 1060 incubated in the light for two weeks with 1 mM Mn(II) without the treatment to remove
 1061 manganese oxides from the inoculum. The untreated biofilms contained dolomite (CaMg(CO₃)₂,
 1062 “2”), manganese oxides (CaMnO₃, “3”), and aragonite (CaCO₃, “4”). Bottom spectrum:
 1064 inoculum treated to remove the carry-over of manganese oxides before any incubation (see
 1065 Methods section 1.1.1) contained sulfur; (S, “5”) and calcium carbonate (CaCO₃, “6”).

1066
 1067
 1068



1069
 1070 **Extended Data Figure 11.** Reticulate history of bacteriochlorophyll biosynthesis genes supports
 1071 a long history of phototrophy in the Chlorobiales stem lineage. Horizontal gene transfers and
 1072 gene duplications of bacteriochlorophyll genes were taken from⁷³, and age estimates for crown
 1073 Chlorobi and GNS groups were taken from²⁸.

1074
 1075

Extended Data Table 1. Aquatic environments with H₂S and Mn in the photic zone.

Water body	H ₂ S (μM)	Mn(II) (μM)	Photic Zone	Reference
Lake A	230	140	Green Sulfur Bacteria	70
Lake Vanda	240	120	Unclear	71
Garrow Lake	20	18	Green Sulfur Bacteria	72
Sombre Lake	1.2	68	Green Sulfur Bacteria	73
Svetloe Lake	2	60	Green Sulfur Bacteria	74
Black Sea	2	8.4	Green Sulfur Bacteria	75
Green Lake	20-30	50-60	Green Sulfur Bacteria	9

Extended Data Table 2. Shake tube and transfer procedures used to obtain enrichments from conditions 1 and 2.

First round shake tube	Incubation period, (days)	Colonies	Transfer into liquid medium	Incubation period (days)	Growth ¹	Enrichment
20 μM Na ₂ S, 1 mM MnCl ₂	30	Black and dark brown	Brown colony; 0.02 mM Na ₂ S, 1 mM MnCl ₂	30	+	Condition 1
1 mM Na ₂ S	30	Black, white and dark brown	Brown colony; 1 mM Na ₂ S	30	+++	Condition 2
Second round shake tube	Incubation period (days)	Colonies	Transfer into liquid medium	Incubation period (days)	Growth ¹	Enrichment
0.02 mM Na ₂ S, 1 mM MnCl ₂	30	Brown, dark brown	Brown colony; 0.02 mM Na ₂ S, 1 mM MnCl ₂	30	+	Condition 1
1 mM Na ₂ S	30	Brown, dark brown	Brown colony; 1 mM Na ₂ S	30	+++	Condition 2

¹Growth of colonies transferred from shake to liquid media of same chemical composition; '+' signifies low microbial growth, '+++’ signifies high microbial growth. ²Microbial composition determined by metagenomic sequencing. ³*Achole*

equifetale, *Alistipes* sp. HGB5, and *Caldicoprobacter oshimai*.

1078

1079

1080

1081

Extended Data Table 3. Summary of the methods used to examine the redox state of manganese in enrichment cultures.

Enrichment condition	Transfer condition	Transfer MFGL medium composition	Incubation time (days)	Growth ¹	Mn oxidation activity ²
Condition 1	Cell suspension	0.02 mM Na ₂ S, 1mM MnCl ₂	3	-	+
Condition 2	Cell suspension	0.02 mM Na ₂ S, 1 mM MnCl ₂	3	-	-
Condition 1	5 % inoculum	0.02 mM Na ₂ S, 1mM MnCl ₂	7	-	-
Condition 2	5 % inoculum	0.02 mM Na ₂ S, 1mM MnCl ₂	7	+	-

¹The + or – indicates visible growth of the co-culture, ²Manganese oxidation in the enrichment cultures was examined using XPS; + or – signifies the presence or absence of Mn(II) oxidizing activity in the microbial co-culture.

1082

Extended Data Table 4. Mn(II) oxidation genes with confirmed function compared using BLASTp v. 2.6.0+ against *Chlorobium limicola* SR-12 genome.

Locus ID	Gene Annotation	Gene Name	Organism	Ref.	% identity
PputGB1_3353	animal heme peroxidase	<i>mopA</i>	<i>Pseudomonas putida</i>	19	46
WP_007817484	animal heme peroxidase	<i>ahpL</i>	<i>Roseobacter</i> sp. AzwK-3b	20	40
WP_009209951	animal heme peroxidase	<i>mopA</i>	<i>Aurantimonas manganoxydans</i>	53	47
WP_006837219	multi-copper oxidase multi-copper oxidase /	<i>mnxG</i>	<i>Bacillus</i> sp. strain SG-1	18	no hits
WP_076798083	billirubin oxidase	<i>boxA</i>	<i>Arthrobacter</i> sp. QXT-31	34	no hits
AFL56752	multi-copper oxidase, type 2	<i>cotA</i>	<i>Bacillus pumilus</i> WH4	77	no hits
CAJ19378	multi-copper oxidase multi-copper oxidase /	<i>moxA</i>	<i>Pedomicrobium</i> sp. ACM 3067	52	no hits
NP_745328	billirubin oxidase	<i>mcoA</i>	<i>Pseudomonas putida</i>	19	no hits
EG12318	multi-copper oxidase	<i>cueO</i>	<i>Escherichia coli</i>	78	no hits

Note: All AHPs also hit hemolysin-type calcium-binding region in *Chlorobium limicola* (E-value 3e-21, bit score 1083)

1083
1084